

NASA Contractor Report 175115

NASA-CR-175115  
19860016379

# Fatigue Crack Layer Propagation in Silicon-Iron

Y. Birol, G. Welsch, and A. Chudnovsky  
*Case Western Reserve University  
Cleveland, Ohio*

May 1986

Prepared for  
Lewis Research Center  
Under Grant NAG 3-223

**LIBRARY COPY**

JUN 12 1986

LANGLEY RESEARCH CENTER  
LIBRARY, NASA  
HAMPTON, VIRGINIA

**NASA**  
National Aeronautics and  
Space Administration



DISPLAY 07/2/1

86N25851\*\* ISSUE 16 PAGE 2608 CATEGORY 39 RPT#: NASA-CR-175115 NAS  
1.26:175115 CNT#: NAG3-223 86/05/00 47 PAGES UNCLASSIFIED DOCUMENT

UTTL: Fatigue crack layer propagation in silicon-iron TLSP: Final Report

AUTH: A/BIROL, Y.; B/WELSCH, G.; C/CHUDNOVSKY, A.

CORP: Case Western Reserve Univ., Cleveland, Ohio. AVAIL. NTIS

SAP: HC A03/MF A01

CIO: UNITED STATES

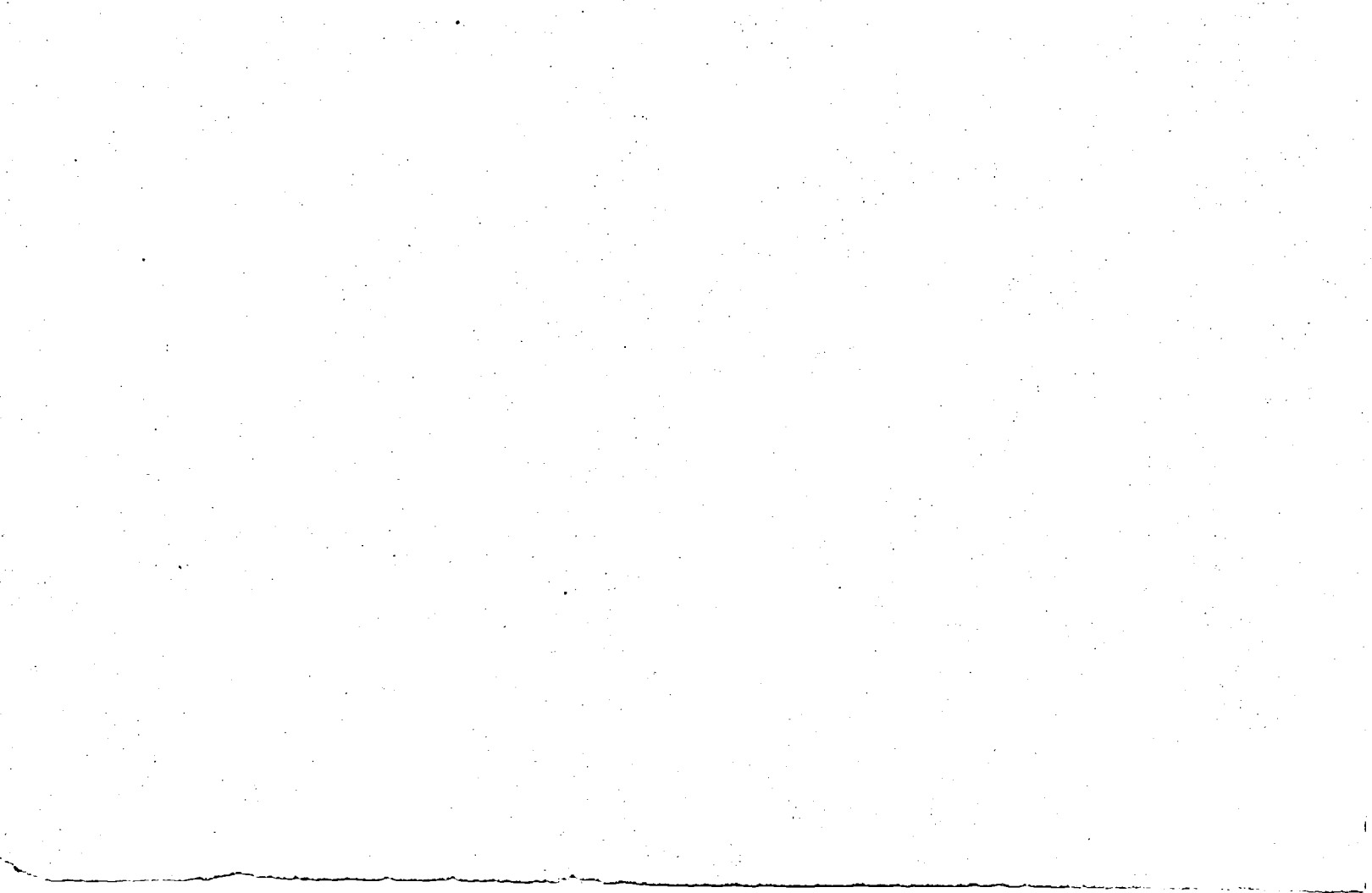
MAJS: /\*CRACK PROPAGATION/\*FATIGUE (MATERIALS)/\*FRACTURE MECHANICS/\*IRON ALLOYS  
/\*PLASTIC DEFORMATION/\*SILICON ALLOYS

MINS: / BRITTLENESS/ ELECTRON MICROSCOPY/ LOADS (FORCES)/ MICROSTRUCTURE/  
TENSILE PROPERTIES

ABA: Author

ABS: Fatigue crack propagation in metal is almost always accompanied by plastic deformation unless conditions strongly favor brittle fracture. The analysis of the plastic zone is crucial to the understanding of crack propagation behavior as it governs the crack growth kinetics. This research was undertaken to study the fatigue crack propagation in a silicon iron alloy. Kinetic and plasticity aspects of fatigue crack propagation in the alloy were obtained, including the characterization of damage evolution.

ENTER:



## CHAPTER I

### INTRODUCTION

Fatigue crack propagation in metals is almost always accompanied by plastic deformation unless the conditions strongly favor brittle fracture. The extent of this plastic deformation depends on testing conditions, specimen geometry and microstructural characteristics of the metal studied. The analysis of the plastic zone is crucial to the understanding of fatigue crack propagation behavior as it governs the crack growth kinetics.

This research was undertaken to study the fatigue crack propagation in a silicon-iron alloy. This alloy with varying Si contents (from 2.5% to 4% Si) has been extensively used in fatigue studies (1-5) as it closely represents the behavior of low and medium strength steels. An attempt was made to characterize the damage evolution.

### EXPERIMENTAL PROCEDURE

The alloy<sup>(\*)</sup> used in this investigation had 2.6 wt. % Si. The as-received material was hot-rolled and pickled and exhibited a heterogeneous grain structure, typical of hot rolled metals. Its tensile properties were evaluated for both transverse and longitudinal directions. Microstructural characteristics and tensile properties are given in Table 1.

---

(\*)Alloy supplied by Republic Steel Corporation, now LTV Steel Corp.

TABLE I.

MATERIAL CHARACTERISTICS

## - PHASE: FERRITE

FERRITE IS THE MOST DUCTILE AMONG THE PHASES IN STEELS.  
IT HAS A SIGNIFICANT AMOUNT OF DEFORMABILITY.

## - HISTORY: HOT ROLLED AND PICKLED.

DUE TO HOT ROLLING, THERE HAS BEEN PARTIAL RECRYSTALLI-  
ZATION WHICH GAVE RISE TO A NONUNIFORM GRAIN STRUCTURE.

## - GRAIN SIZE:

	MEAN INTERCEPT LENGTH, $\mu\text{m}$
LONGITUDINAL DIR.	72
TRANSVERSE "	53
NORMAL "	31

	MAXIMUM	MINIMUM, $\mu\text{m}$
LENGTH	2000	10
WIDTH	300	10
THICKNESS	80	5
	TRANSVERSE	LONGITUDINAL

- YIELD STRESS: 517 MPa. 482 MPa.

- ELASTIC MODULUS:  $2.31 \times 10^5$  MPa.  $1.96 \times 10^5$  MPa.

Figure 1 illustrates geometry of the specimen used in fatigue crack propagation studies. The specimens were mechanically polished prior to fatigue testing to obtain a mirror surface to be able to observe the damage evolution during fatigue crack propagation. No attempt was made to study the initiation of cracks, therefore accelerated conditions were used to initiate the cracks. Fatigue tests were conducted in laboratory air with a servo-hydraulic MTS machine. Crack propagation was monitored with a

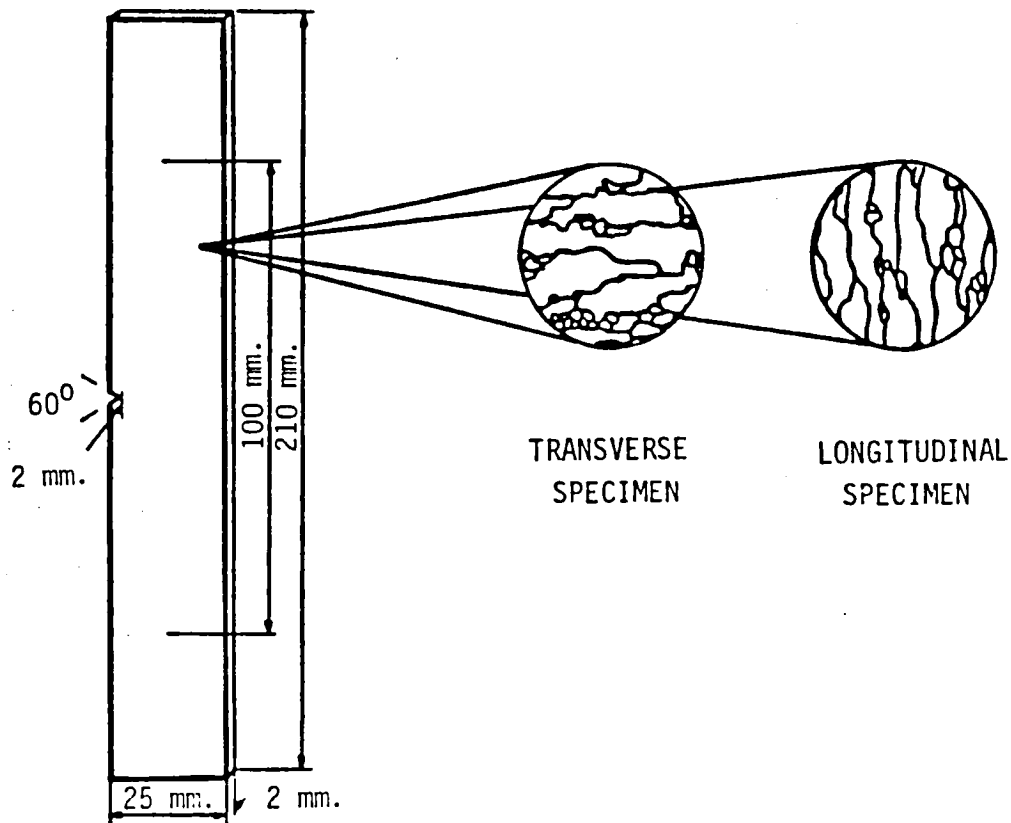


Figure 1. Specimen geometry

traveling microscope and was recorded on a video tape using a camera attached to the microscope. Specimens were cycled in tension-tension, at a frequency of 5 Hz with an R ratio of 0.1 at two different maximum load levels:  $P_{max} = 0.6 P_y$ ,  $0.4 P_y$ .  $0.6 P_y$  was used as the maximum load for acceleration of crack initiation in all tests. An X-Y recorder was employed to record load vs. displacement curves during the test.

Fracture surfaces were examined with both optical and scanning electron microscopy. The side surfaces were also examined to characterize the shape and size of the surface plasticity. An evaluation of the through-thickness plastic zone is reported in Chapter III.

## CHAPTER II

### CRACK LAYER CHARACTERIZATION

Kinetics of stable crack growth in longitudinal and transverse specimens for two different maximum load levels are plotted in Figure 2. There is not much difference between longitudinal and transverse directions as far as growth kinetics is concerned. It should be noted that tensile properties along and perpendicular to the rolling direction are not significantly different either. Longitudinal specimens which have a slightly lower yield stress and elastic modulus exhibit slightly higher crack growth rates.

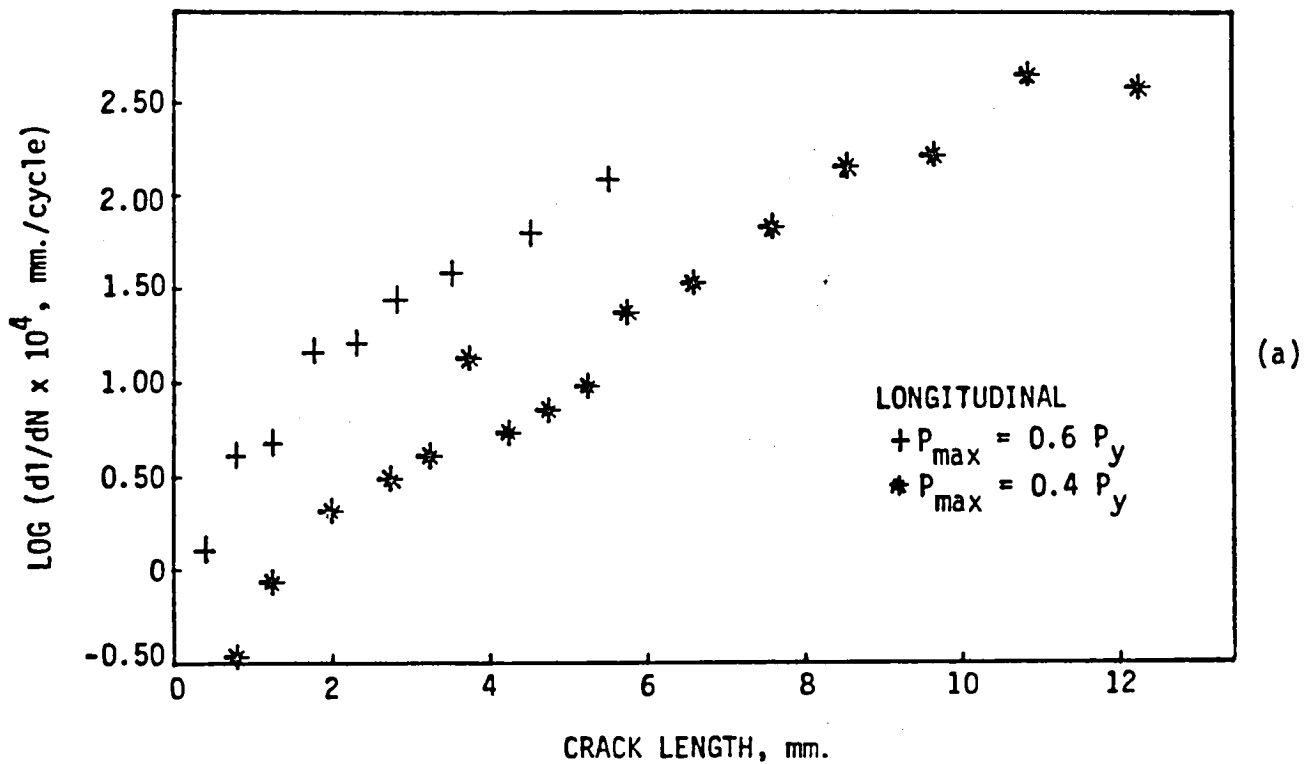


Figure 2. Crack growth kinetics of (a) longitudinal and (b) transverse specimens.



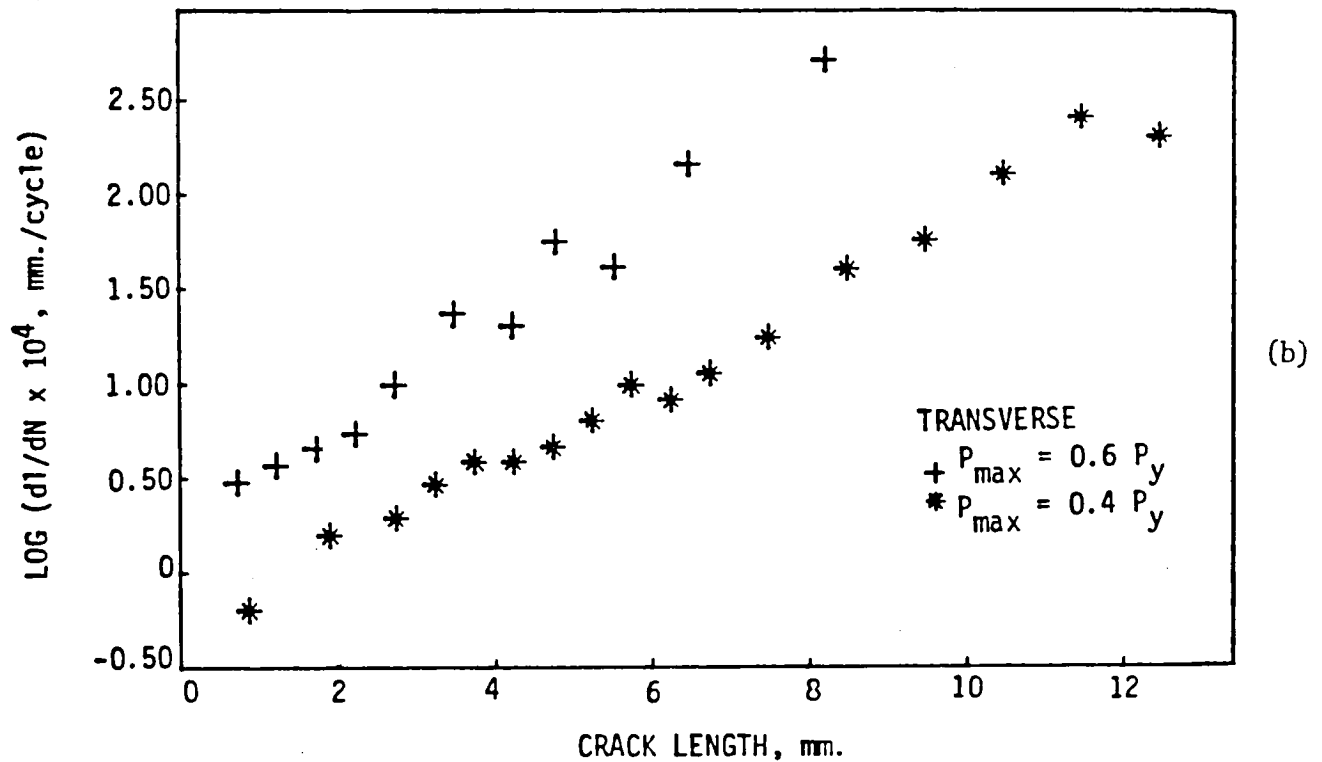


Figure 2, cont'd.

The variation of width and length of the plastic zone as a function of crack length is illustrated in Figures 3-4. The plots clearly show the extent of plastic deformation that accompanies crack growth. The width of the plastic zone for longitudinal and transverse specimens is not significantly different whereas the length (this is not the length of the zone along crack axis) shows a noticeable difference.

Examples of damage evolution during crack propagation are shown in Figure 5 for two longitudinal specimens fatigued at different stress amplitudes. As can be seen from these sketches the plastic zone expands

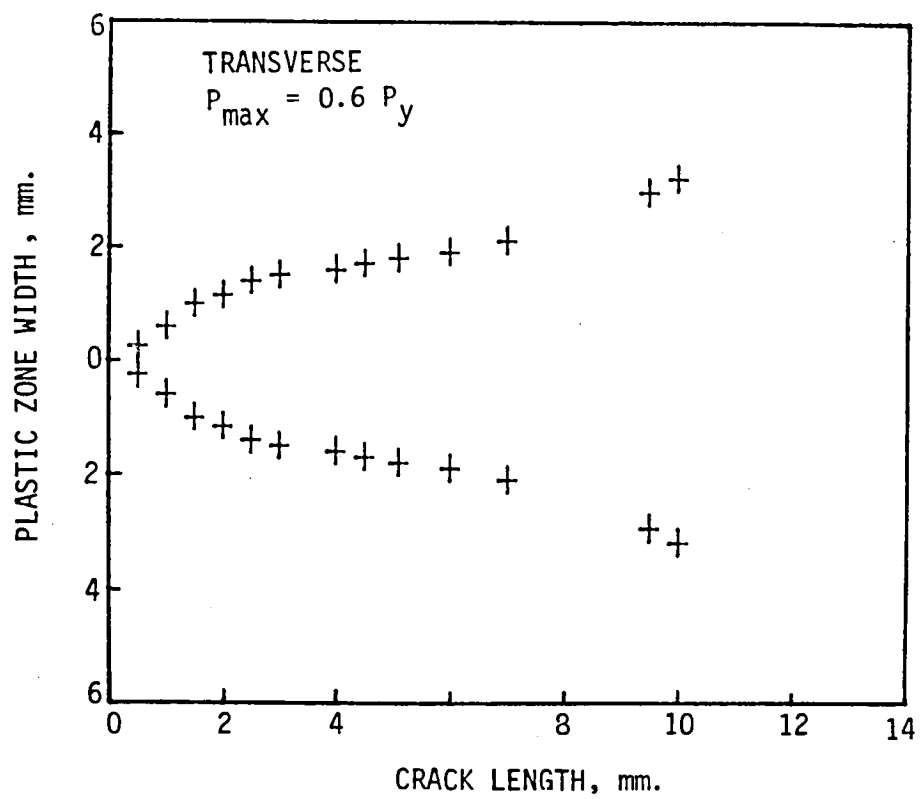
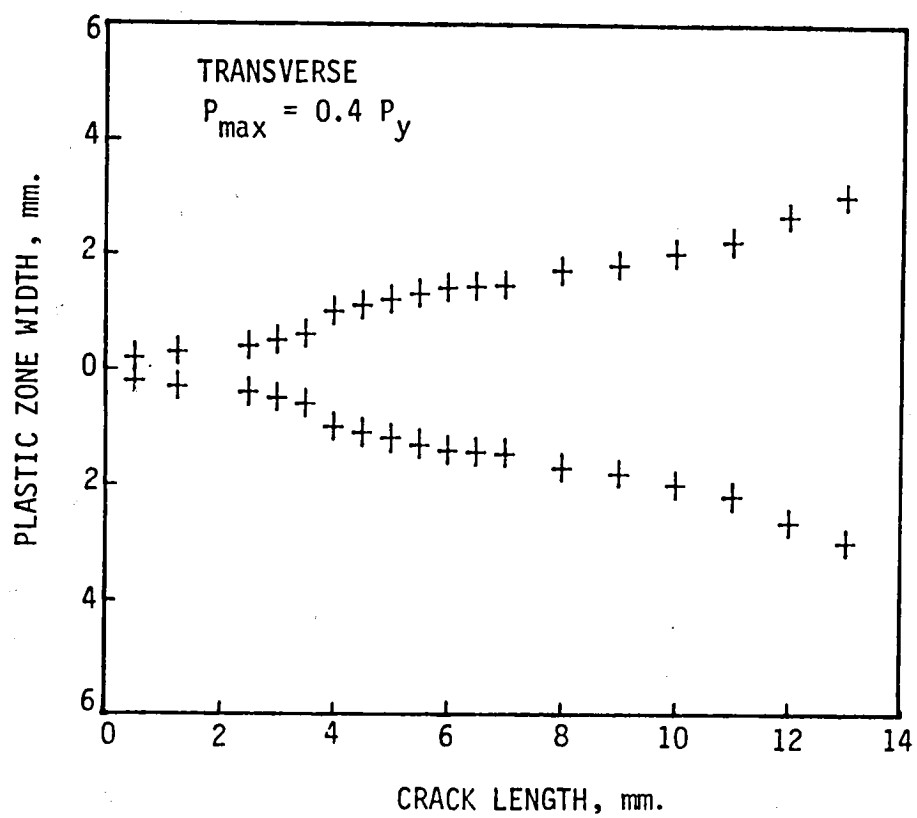


Figure 3. Variation of plastic zone width with crack length.

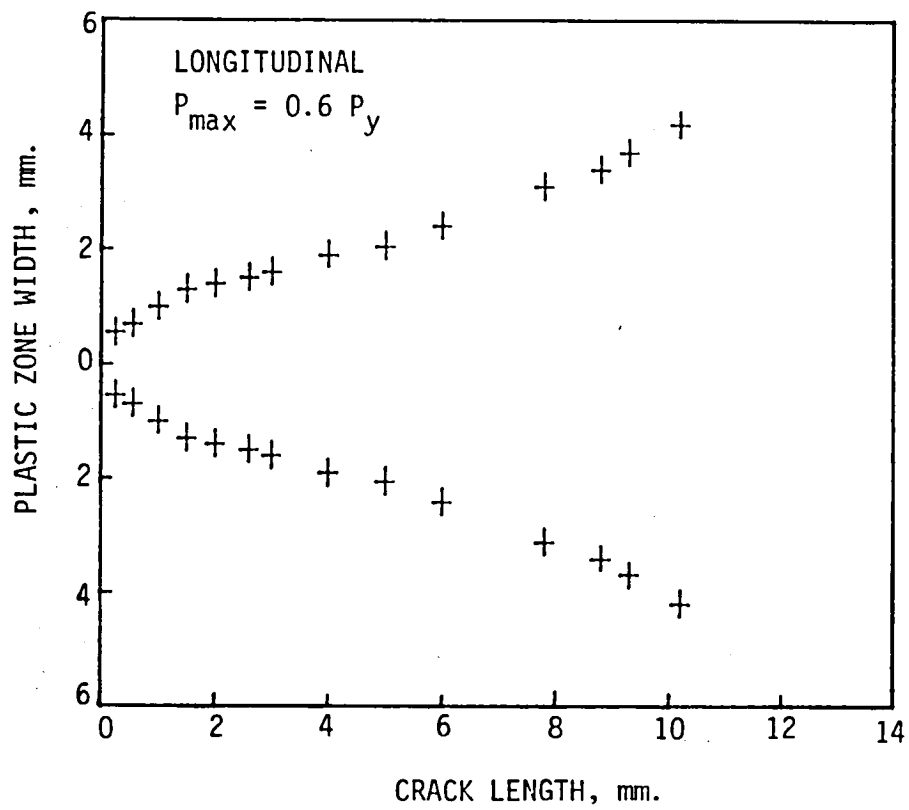
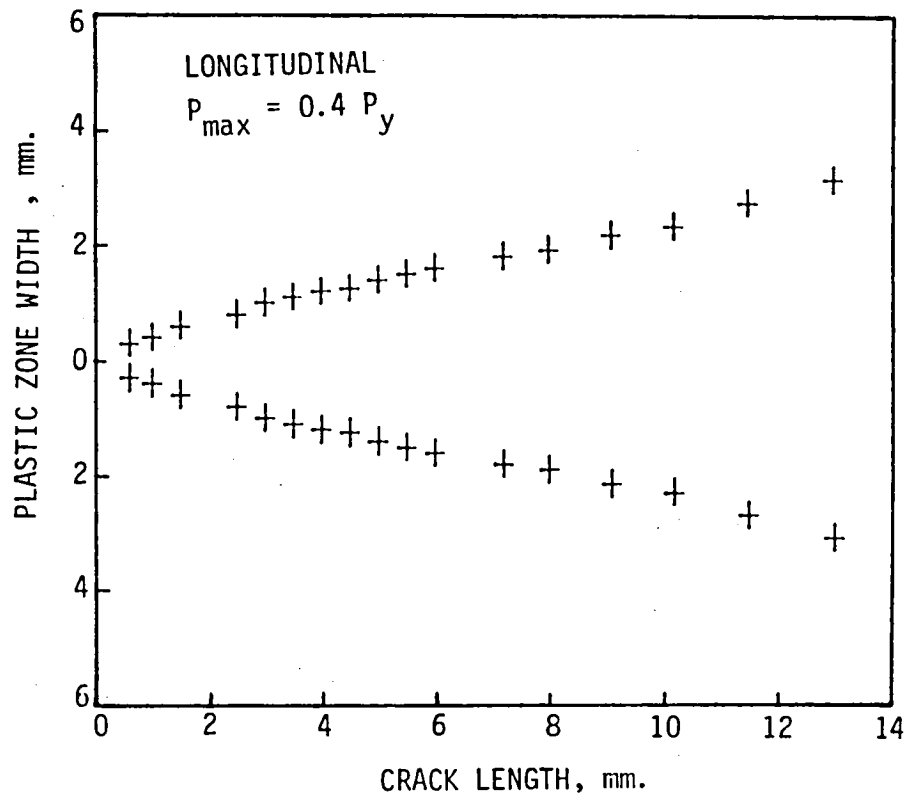


Figure 3, cont'd.

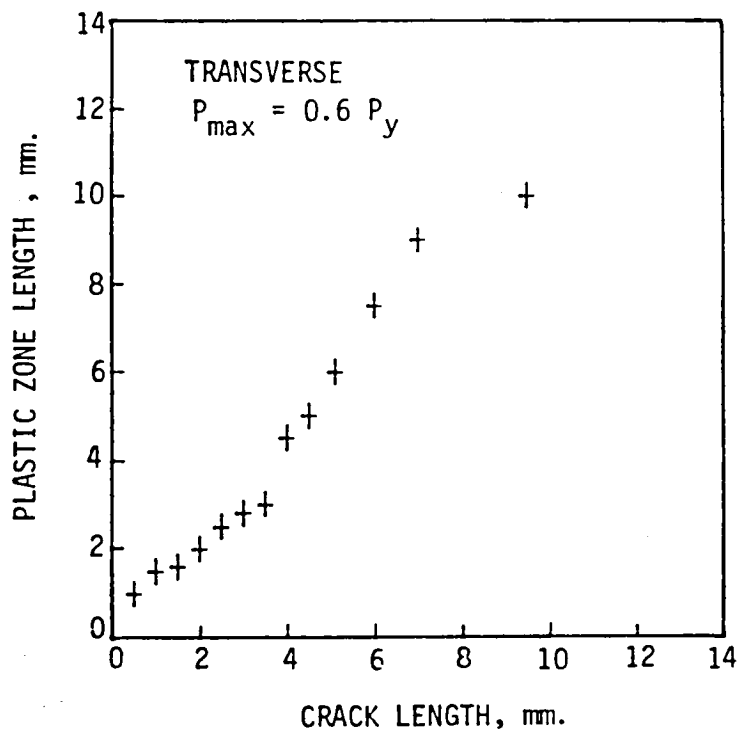
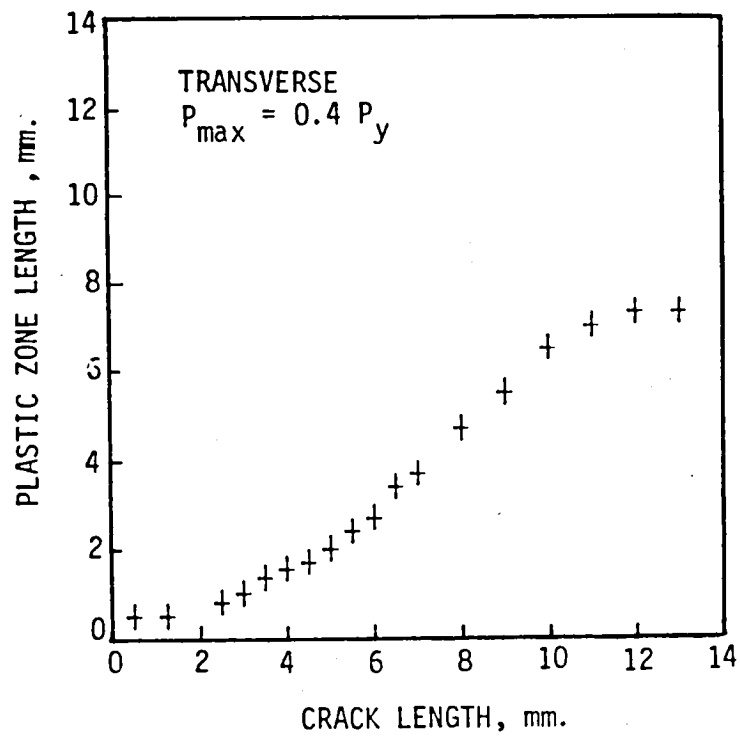


Figure 4. Variation of plastic zone length with crack length.

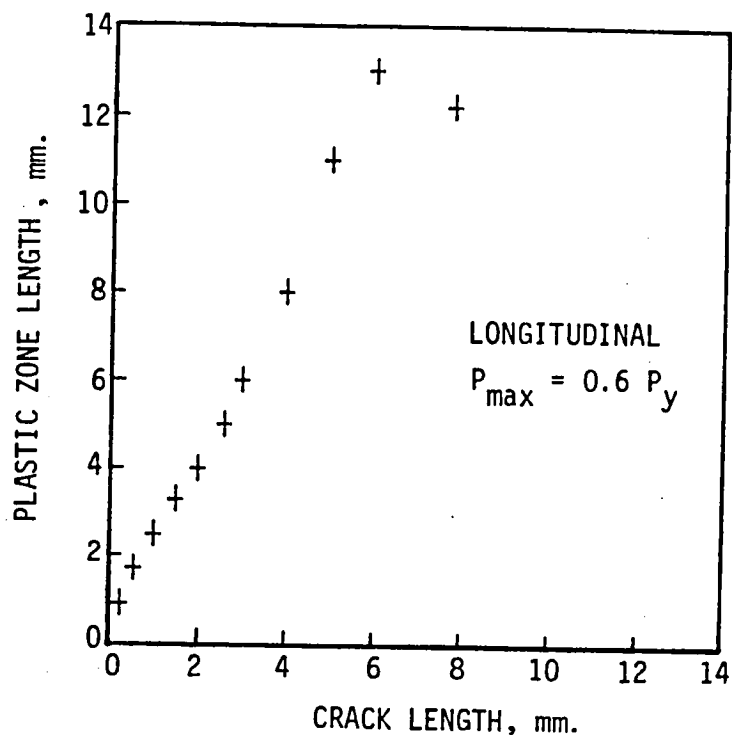
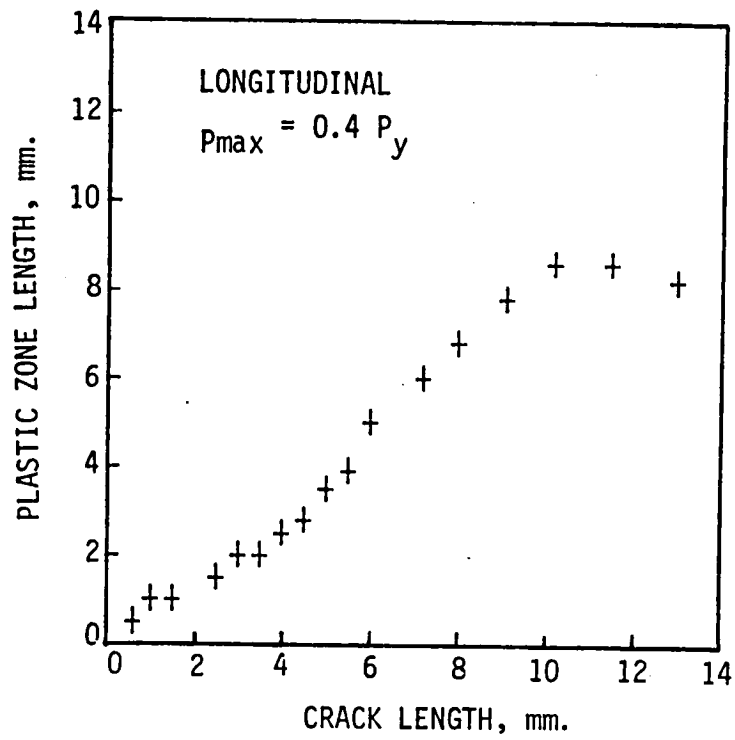


Figure 4, cont'd.

and changes shape as the crack grows. Expansion coefficient and distortion parameter are given by

$$e = \ln (\pi L_p W_p / 4)^{1/2} \quad (1)$$

$$I_2 = \ln (L_p / W_p)^{1/2} \quad (2)$$

where  $l_p$  is the length and  $w_p$  is the width of the plastic zone (6) and are plotted as a function of crack length in Figures 6 and 7.

Energy release rates were also evaluated, using the load displacement curves recorded during fatigue crack propagation. The variation of energy release rate with crack length is illustrated in Figure 8. Energy release rate at a given crack length is found to be higher when crack propagation is accompanied by larger plastic zone.

The fracture surfaces of both transverse and longitudinal specimens showed increasing evidence of cleavage with increasing crack length, particularly along the mid-thickness. The side surfaces were examined with both optical and scanning electron microscopy. The roughness that develops during crack propagation is illustrated in Figure 9.

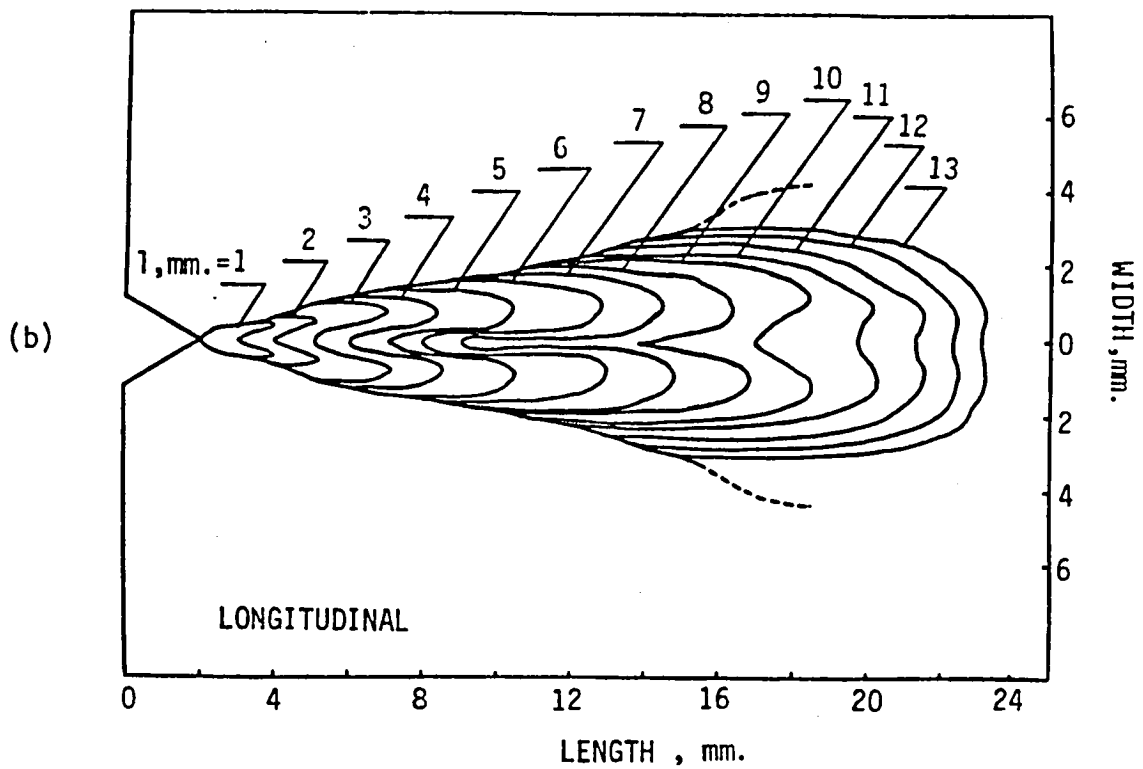
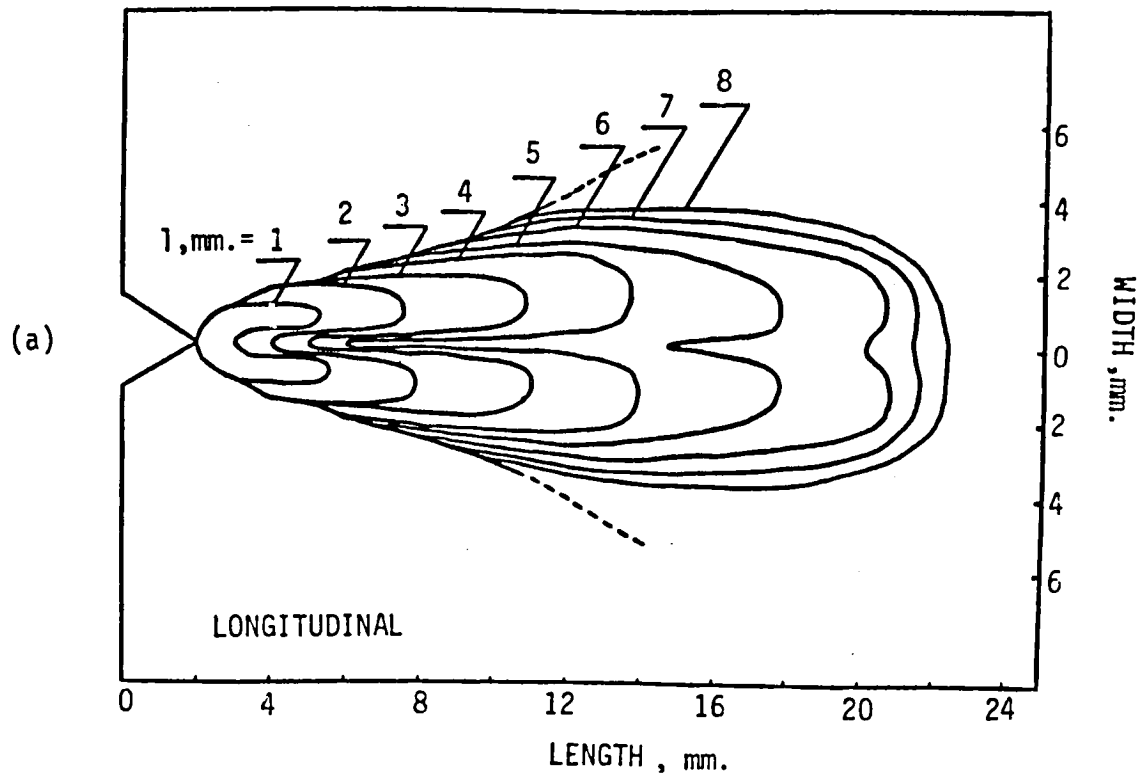


Figure 5. Damage evolution under (a)  $P_{\max} = 0.6 P_Y$ , (b)  $P_{\max} = 0.4 P_Y$  propagation conditions.

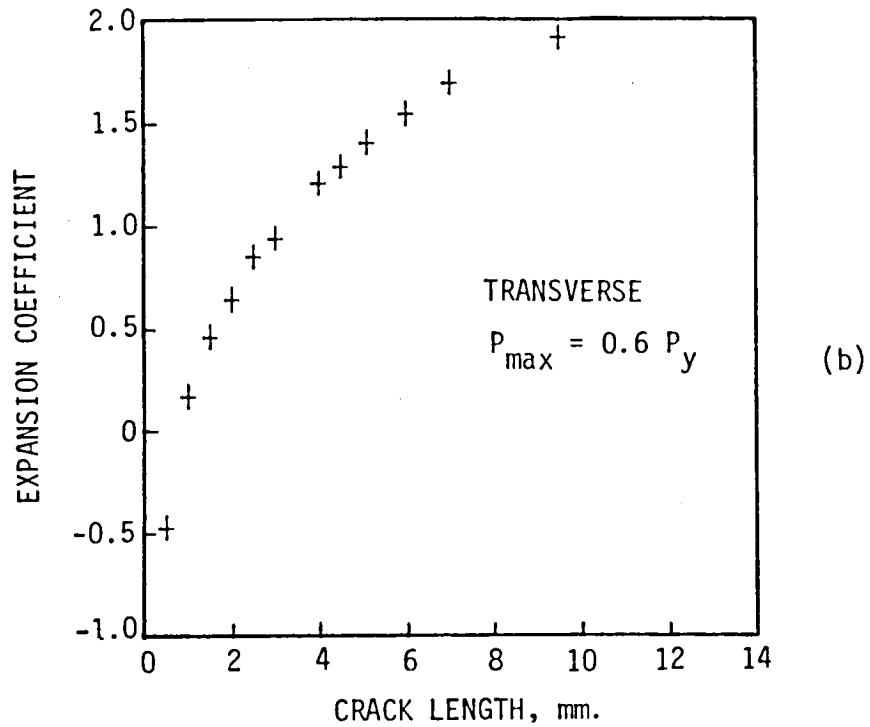
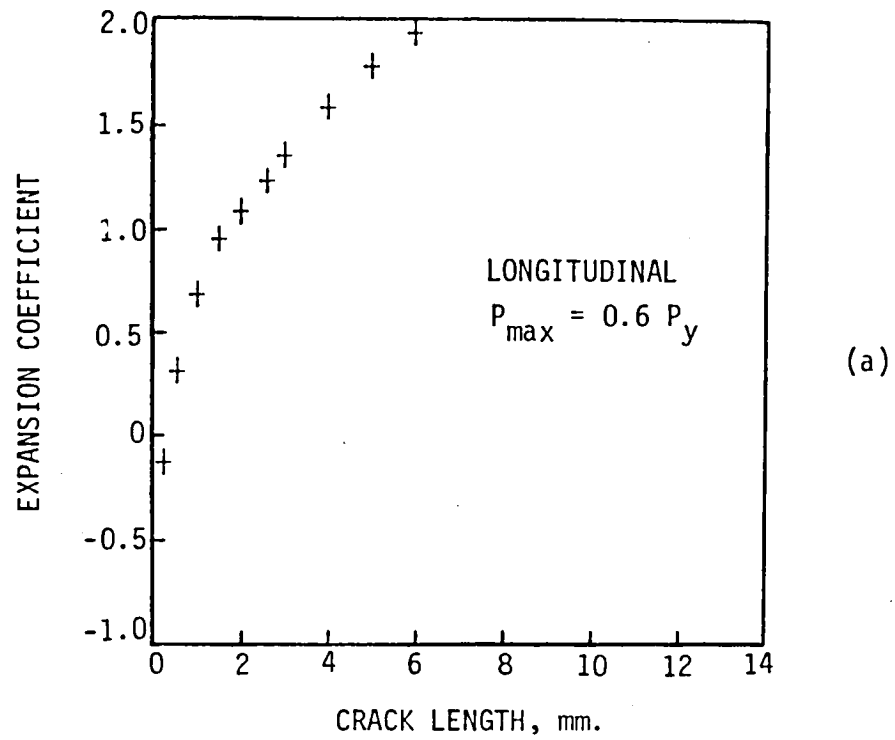


Figure 6. Variation of expansion coefficient with crack length at  $P_{\max} = 0.6 P_y$  for (a) longitudinal, (b) transverse and at  $P_{\max} = 0.4 P_y$  for (c) longitudinal, (d) transverse specimens.



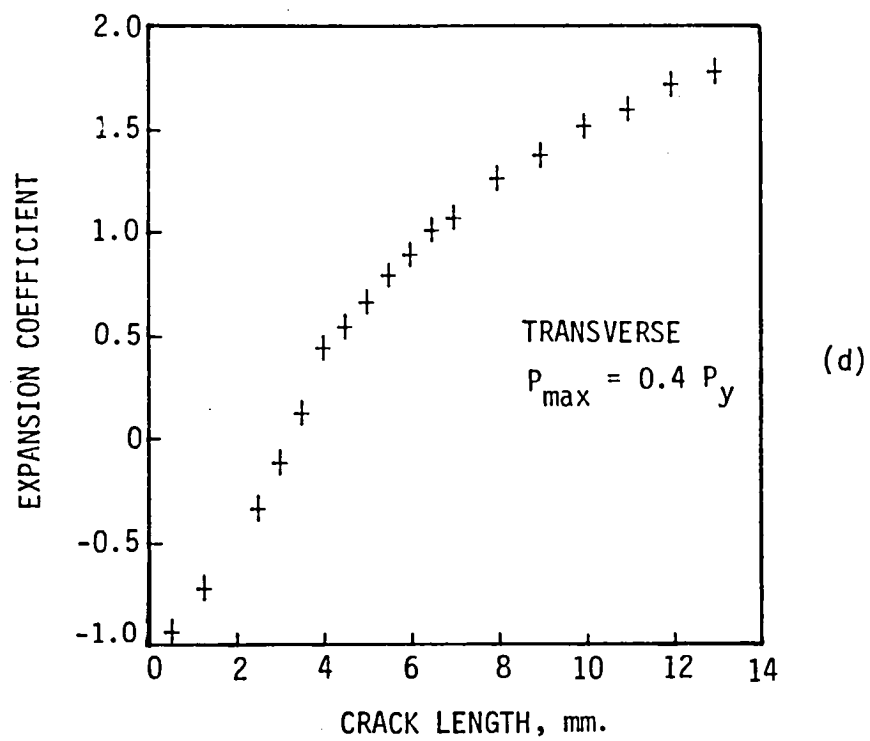
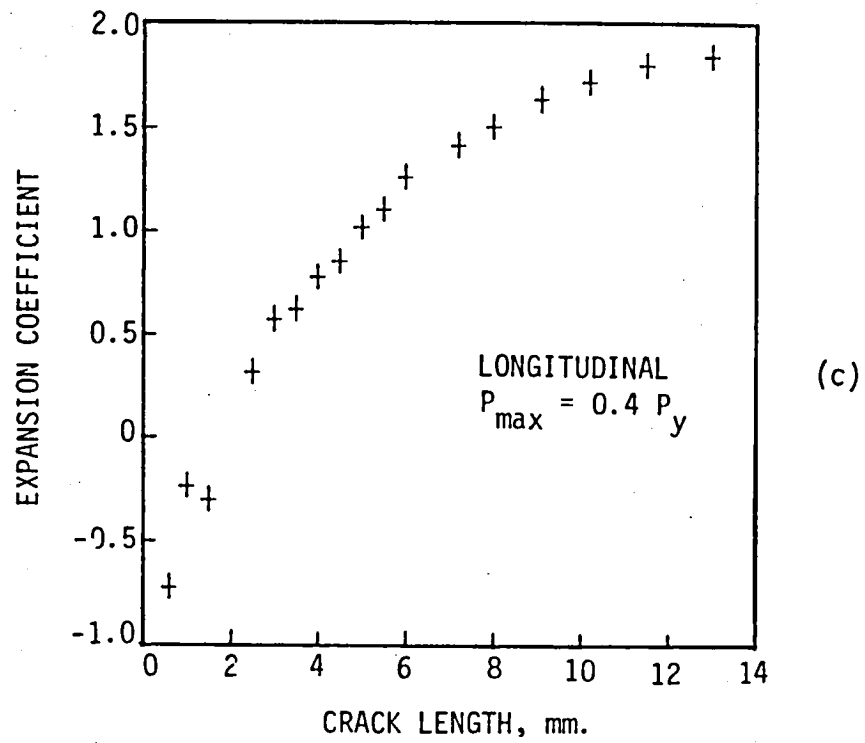


Figure 6, cont'd.

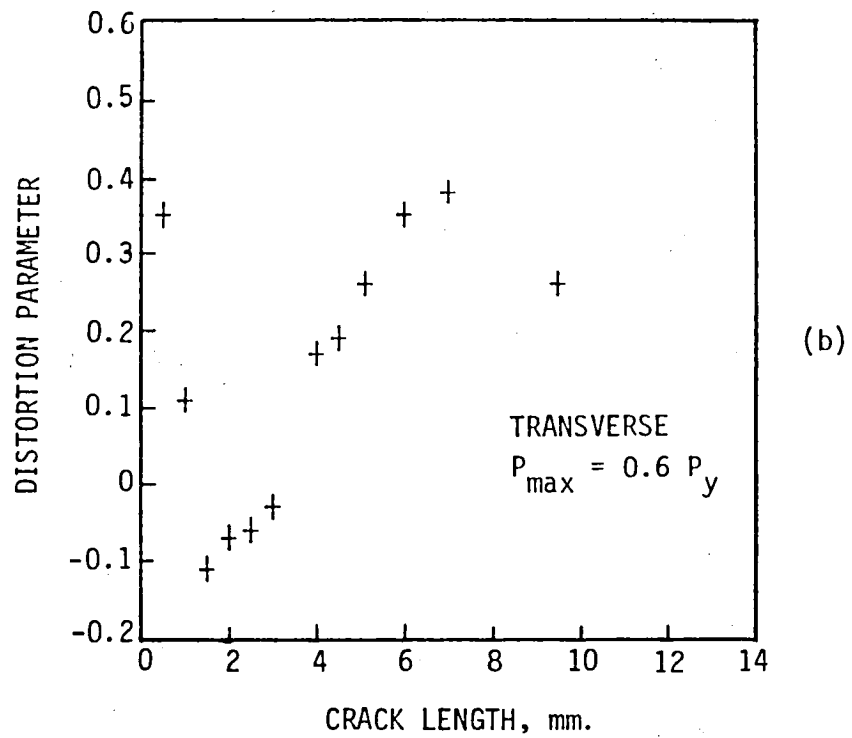
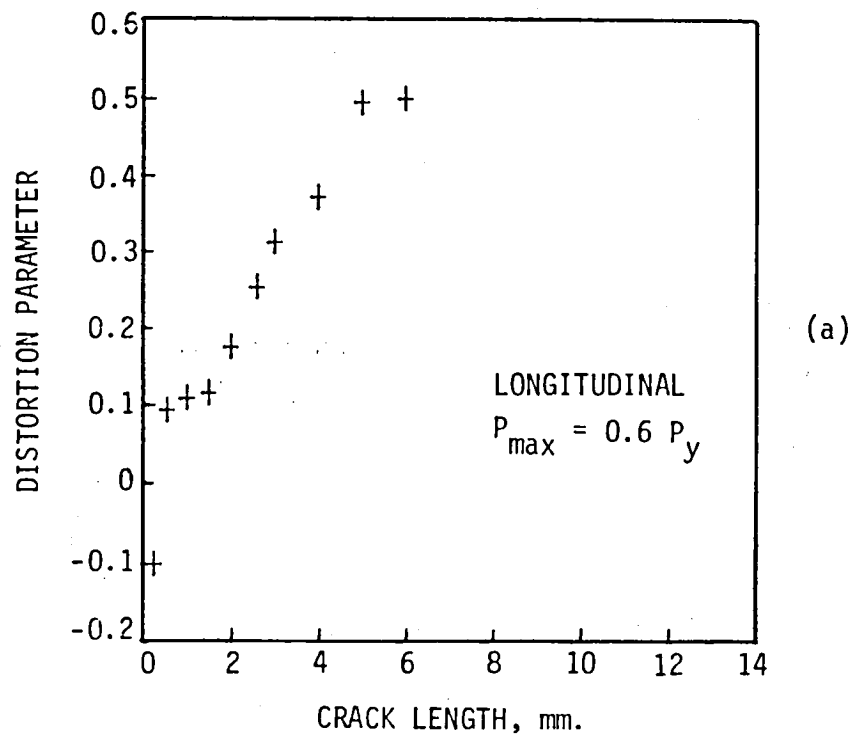


Figure 7. Variation of distortion parameter with crack length at  $P_{\max} = 0.6 P_y$  for (a) longitudinal, (b) transverse and at  $P_{\max} = 0.4 P_y$  for (c) longitudinal, (d) transverse specimens.

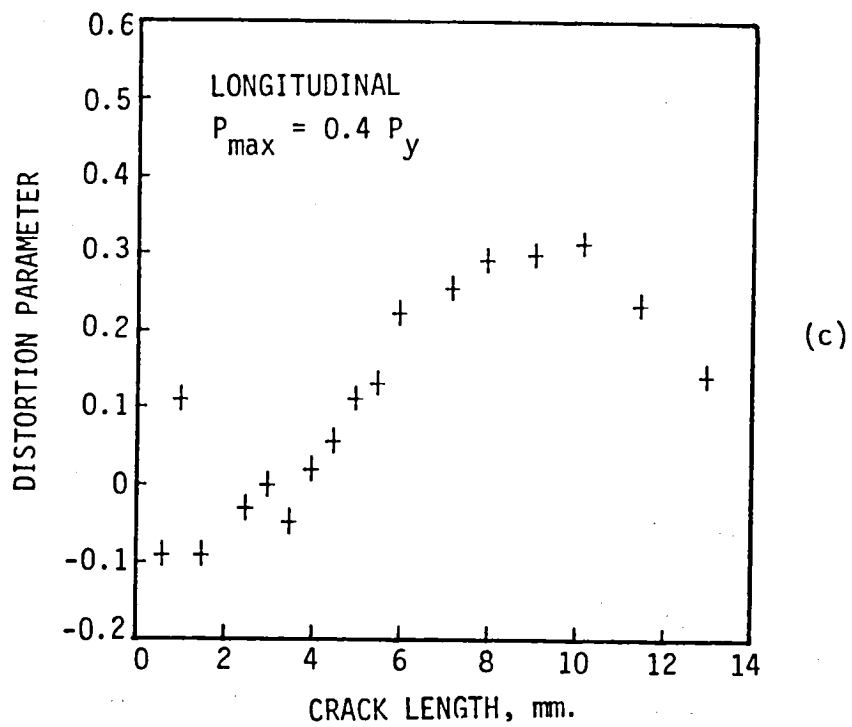
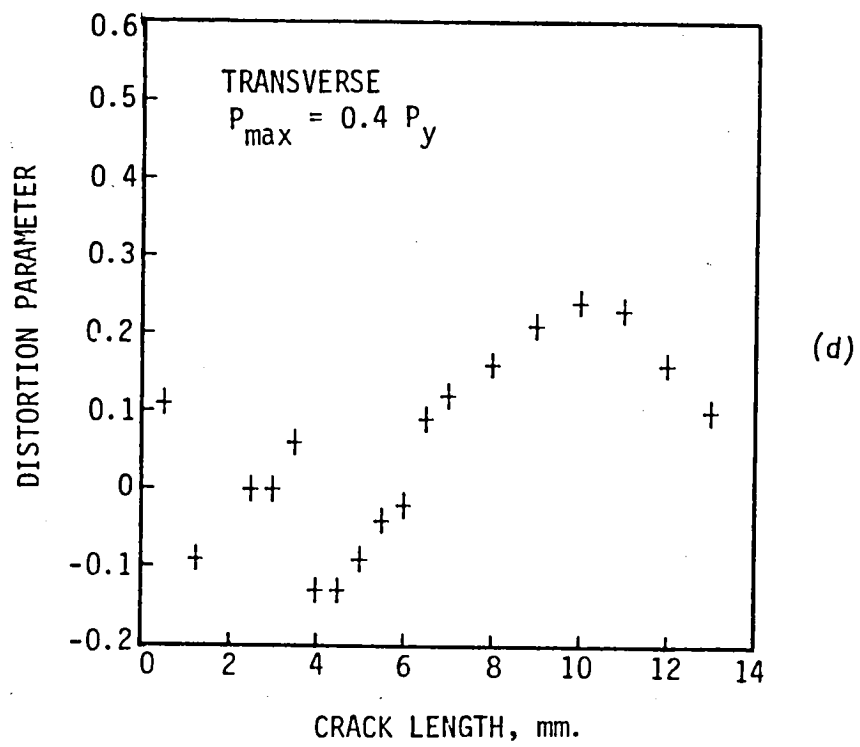


Figure 7, cont'd.

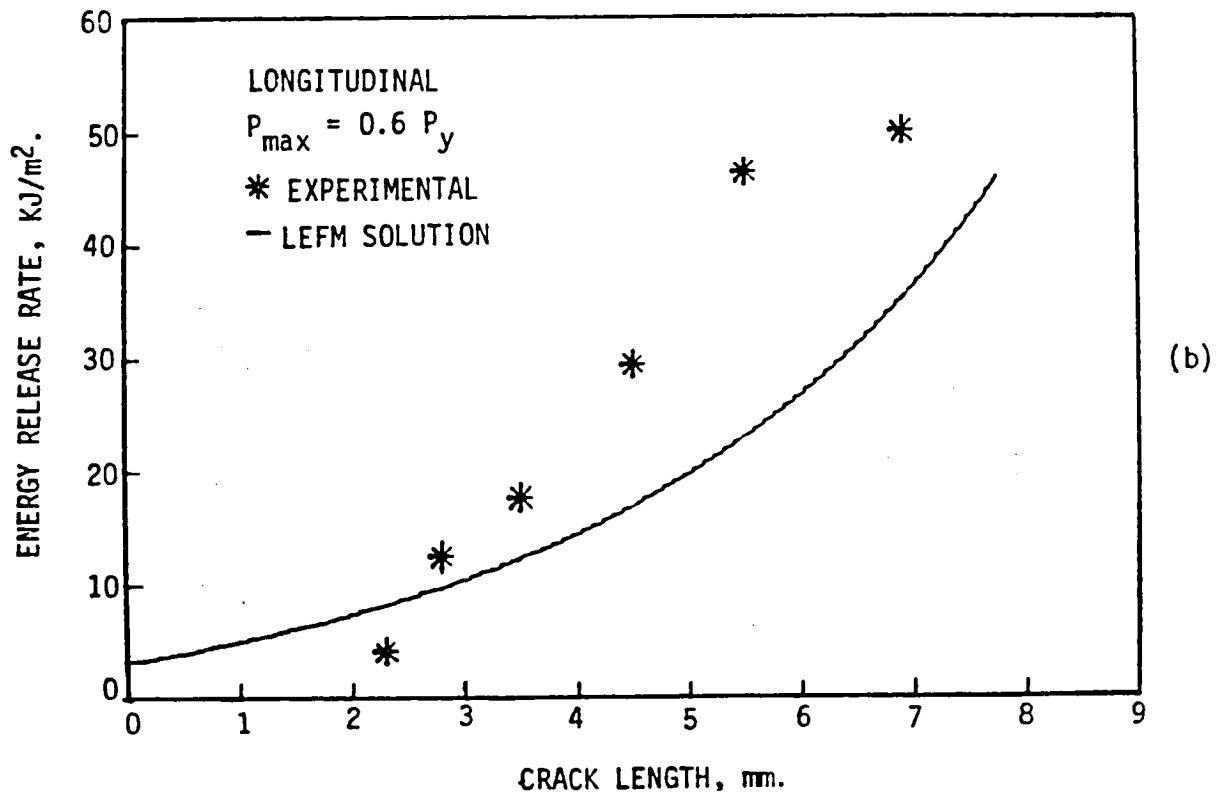
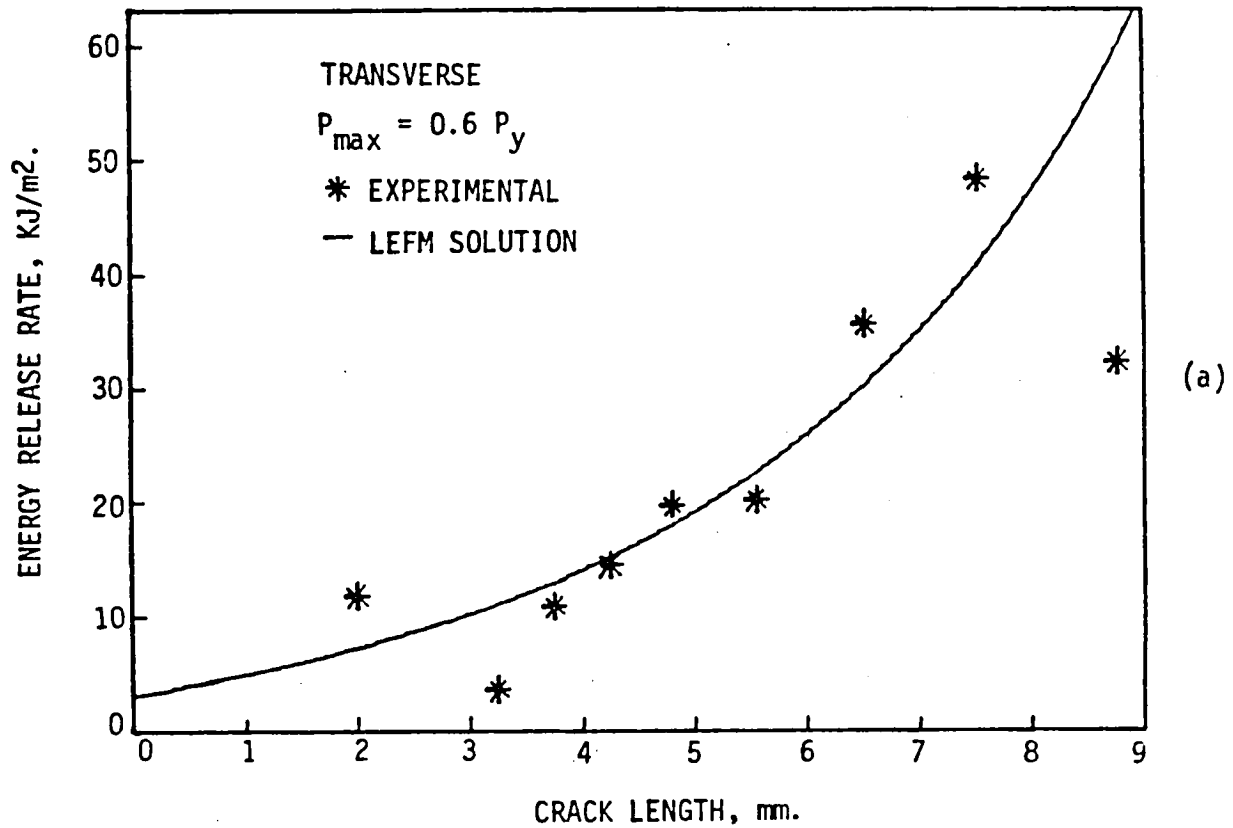


Figure 8. Energy release rate as a function of crack length: (a) Transverse,  $P_{\max} = 0.6 P_y$ ; (b) Longitudinal,  $P_{\max} = 0.6 P_y$ ; (c) Transverse,  $P_{\max} = 0.4 P_y$ ; (d) Longitudinal,  $P_{\max} = 0.4 P_y$ .

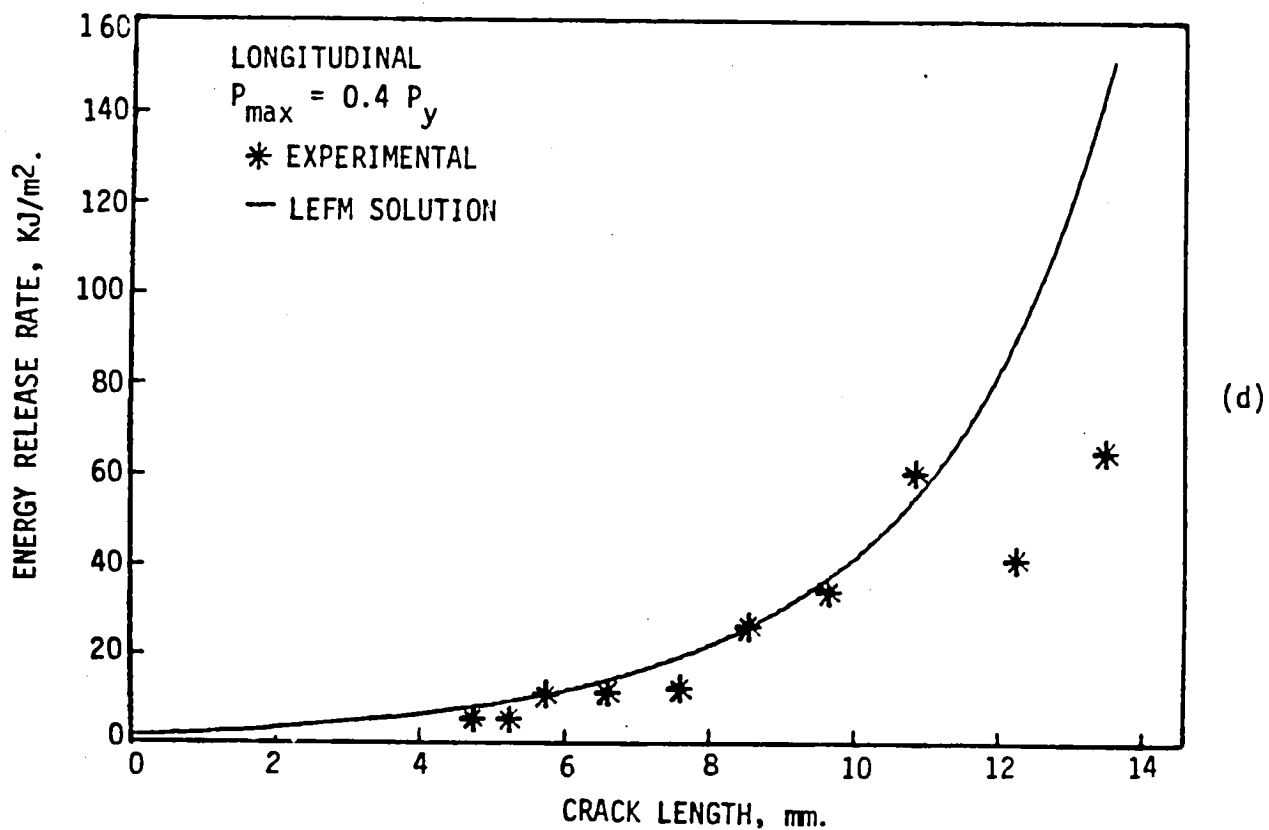
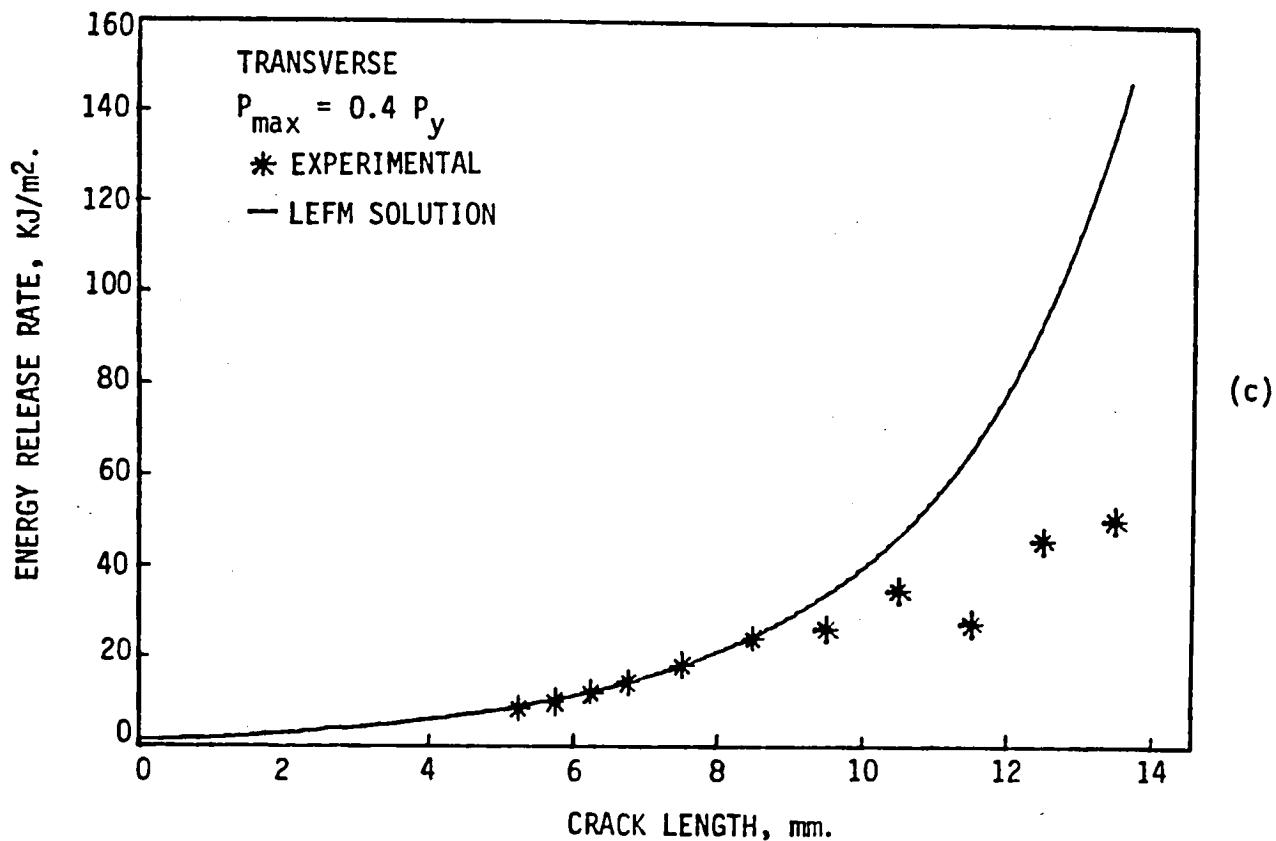
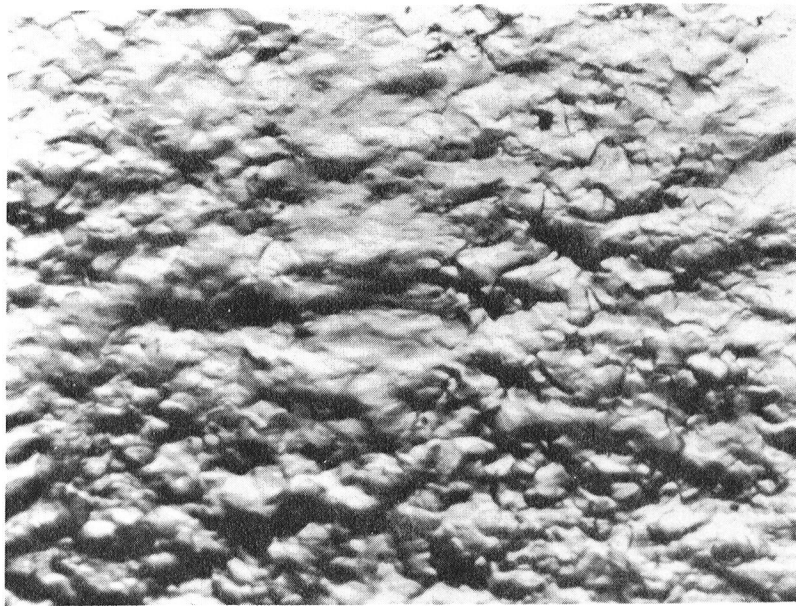
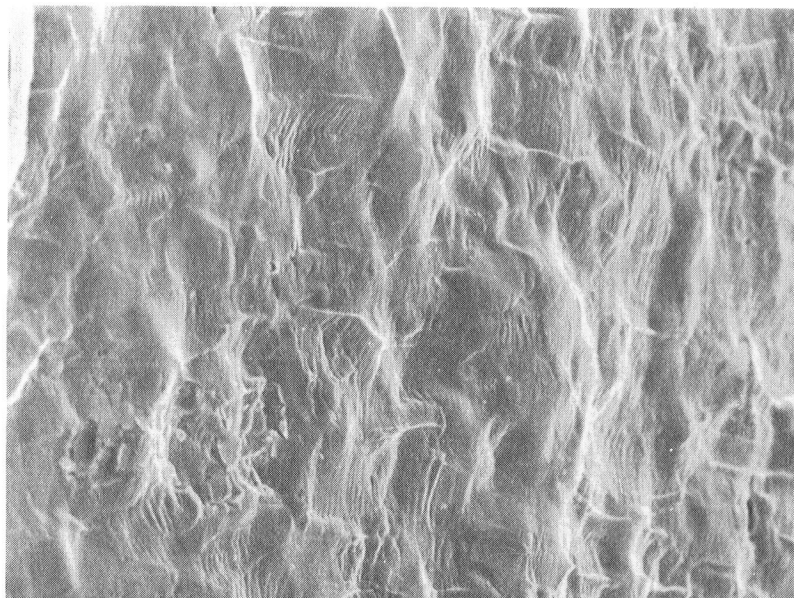


Figure 8, cont'd.



a



b

Figure 9. (a) Optical, (b) SEM micrographs of surface damage introduced by fatigue crack propagation.

## CHAPTER III

### PLASTIC ZONE CHARACTERIZATION

The geometrical characterization of the plastic zone is easy to perform on the surface, but it represents only the plane stress condition. Stress state gradually changes through the thickness, from plane stress to plane strain, and theory predicts that the zone size decreases gradually until it reaches that of plane strain condition at mid-thickness. It is therefore necessary to use other techniques to examine experimentally the plastic zone through the thickness. Most of these techniques can be applied directly to cross sections perpendicular to the fracture surface and crack growth directions.

There are several techniques which can be applied to the study of plastic zones, and those which were employed in this project are discussed below.

### MICROHARDNESS MEASUREMENTS

Change in the hardness can be an indicator of the plastic deformation experienced by the material. Consequently, microhardness has been used as a tool to measure plastic zone size by some investigators (7-11). There is one condition which has to be satisfied for this method to be effective: Material to be studied must either work-harden or work-soften, if any change in hardness is to be detected after fatigue. Austenitic and maraging steels are examples of work-hardening and softening materials, respectively.

Geometrical characterization of the plastic zone can be readily carried out by hardness measurements on fatigued specimens as illustrated

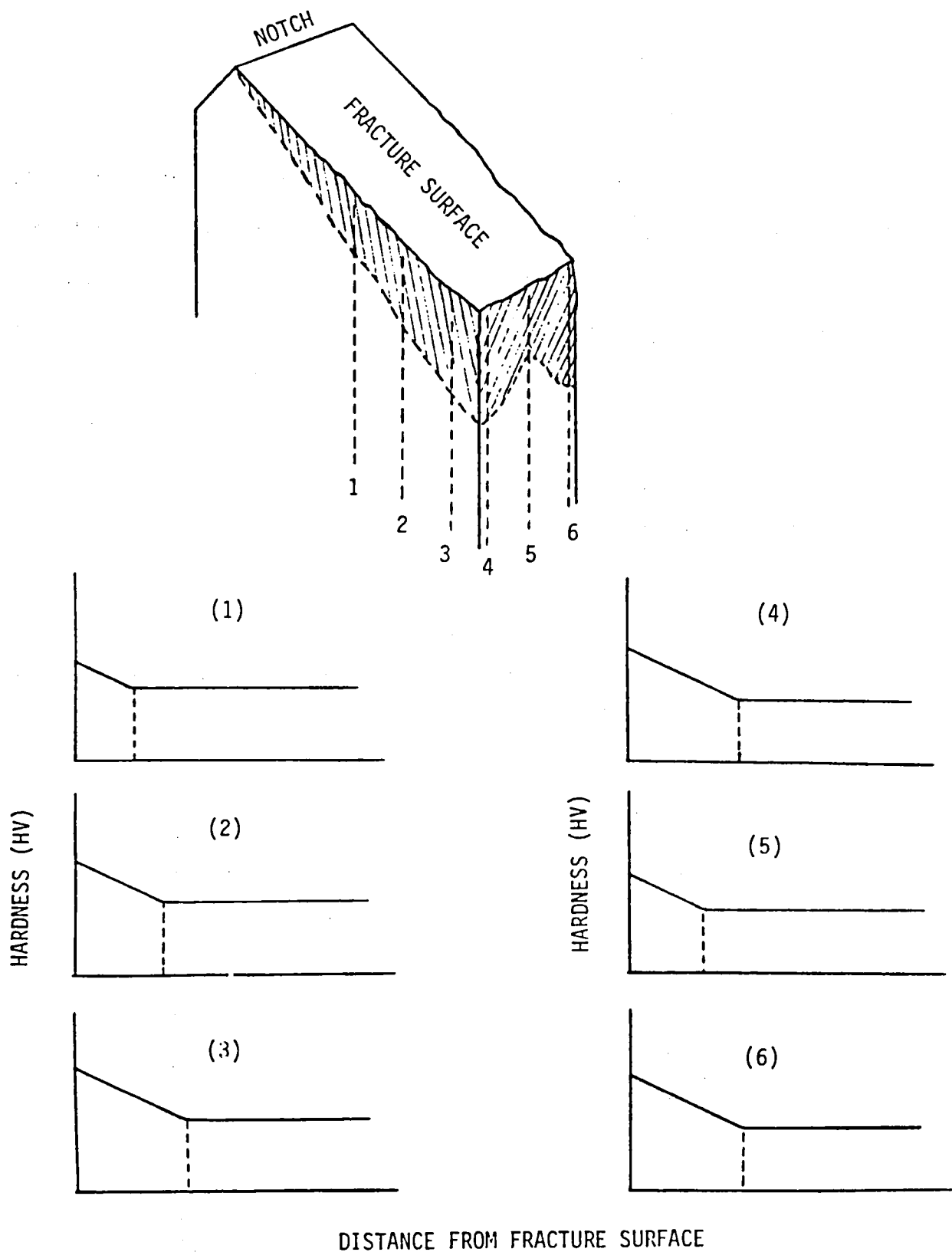


Figure 10. Application of hardness tests on fatigued specimens for geometrical characterization of plastic zones.



in Figure 10. Unfortunately, hardness is not very sensitive to small changes of plastic strain. Therefore, careful standardization is required if damage density is to be obtained.

For this method to be properly applied, the following should be considered: Indentations must be sufficiently large to minimize the error in measurements of indentation size. However, they should also be spaced closely together for an accurate determination of plastic zone boundary. Because the plastic field of an indentation itself strain-hardens the material around it, there is a limit to how close indentations can be placed. Two indentations must be apart by about four to five times the diagonal or diameter. Hence, small loads should be used to produce small indentations. As a result, one should find an optimum indentation size, i.e. optimum load.

Hardness measurements were carried out on cross sections of fatigue specimens, perpendicular to fracture surface and crack propagation direction. A load of 50 g. was used. The same tests were performed on side surfaces.

Hardness, as mentioned earlier, can be an indicator and even a measure of plastic deformation. It is a material property for given conditions. However, it should be kept in mind that a hardness reading is representative only of a small area from which it is taken. Therefore the homogeneity of the material plays an important role and the size of the indentation is significant in hardness testing.

In order to determine plastic zone boundary very precisely and to minimize error in measurements without violating hardness testing rules, 50 g was used as the testing load. This load produced indentations of about  $18 \pm 3$  m (diagonal). This is comparable to and in most cases even

smaller than the mean intercept length of the grain structure.

Hardness measurements on as received material along different directions are shown in Figure 11. The values reported are averages of 12 readings in each case. Hardness varies in a range of as much as 100 vicker units. For vertical cross sections of fatigued specimens, hardness tests were carried out systematically to detect gradients. The surface observations of the plastic zones served as boundary conditions which were used in the justification of the hardness readings on cross sections. We know that the extent of plasticity in the interior of the specimen can not exceed that at the free surface. Figure 10 illustrates the expected gradients. Hardness readings on cross sections at different distances from the notch (increasing crack length) are shown in Figures 12 - 13. Hardness

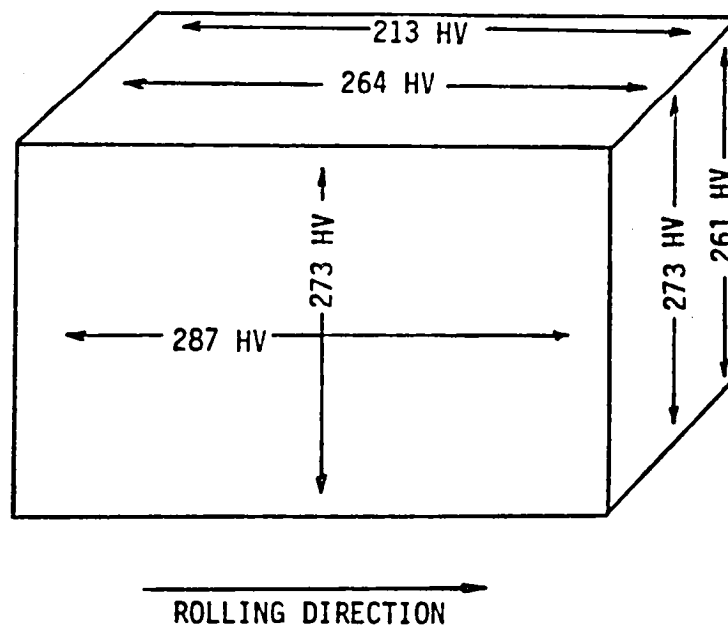


Figure 11. Average hardness distribution on as-received material.

increases in general as we go away from the notch both along mid-thickness and along the edge. No apparent gradients can be defined for short crack lengths and the hardness fluctuates significantly in most cases. The average hardness levels are slightly different from those of the as received material. Hardness gradients develop as distance from the notch, i.e. crack length, increases, as shown in Figures 12, 13. However, in most cases, the hardness distribution exhibits a great deal of variation within very short distances.

The hardness tests carried out on the side surface also exhibit similar characteristics except in a few cases where a certain pattern can be observed which may correlate with the roughness that develops on the surface during fatigue crack propagation. An example is illustrated in Figure 14.

The hardness measurements do not yield consistency for an accurate determination of the plastic zone boundary, although in some cases general conclusions can be drawn from the plots. This can be explained by the non-uniform nature of the structure. Hot rolling has produced partial recrystallization. Consequently some grains are strain-free and soft and some are deformed and hard. Since the indentations are small with respect to the average grain size, the hardness distribution in most cases is a reflection of partial recrystallization both in as received and fatigued conditions. As will be discussed later, annealing heat treatment smoothens the hardness distribution and narrows down the range within which hardness fluctuates, by allowing further recrystallization.

#### ETCHING STUDIES

Etching technique relies on the fact that dislocations multiply rapidly as the metal undergoes plastic strain. The point where a

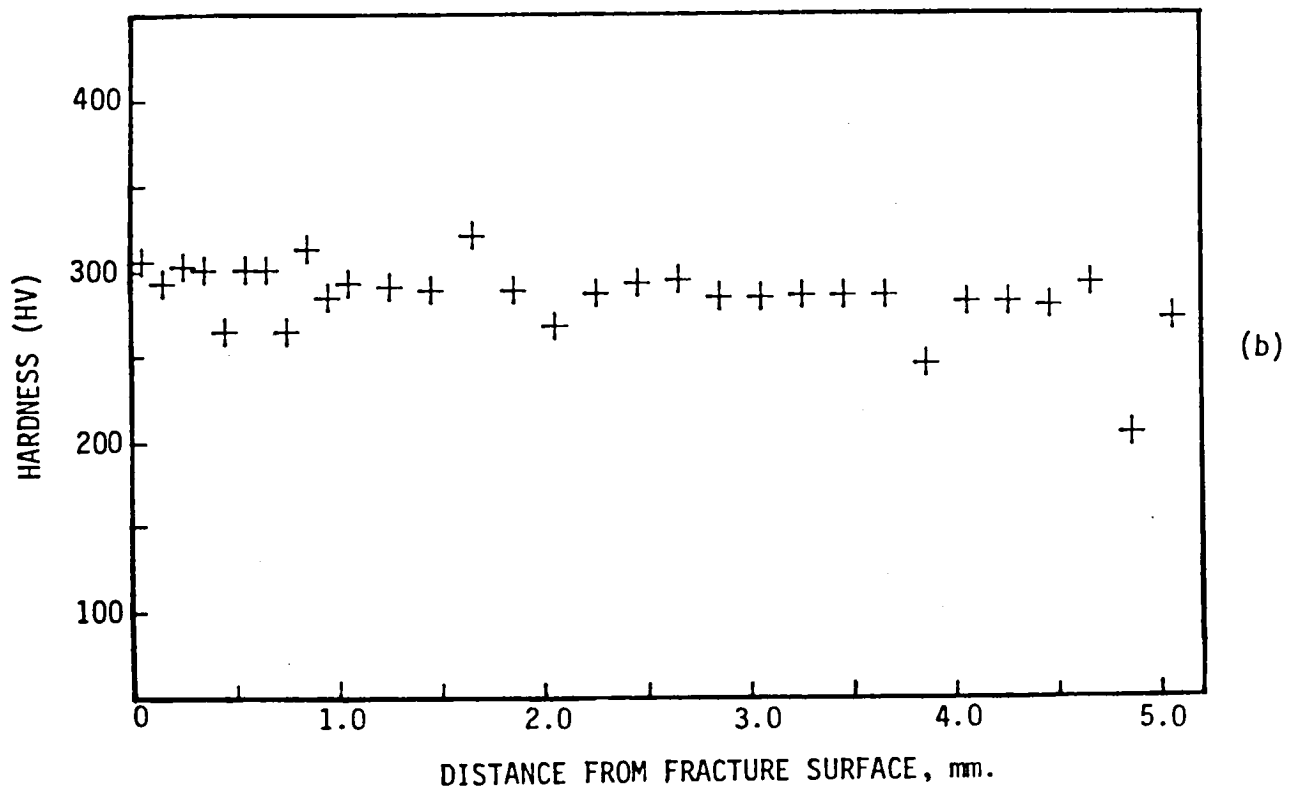
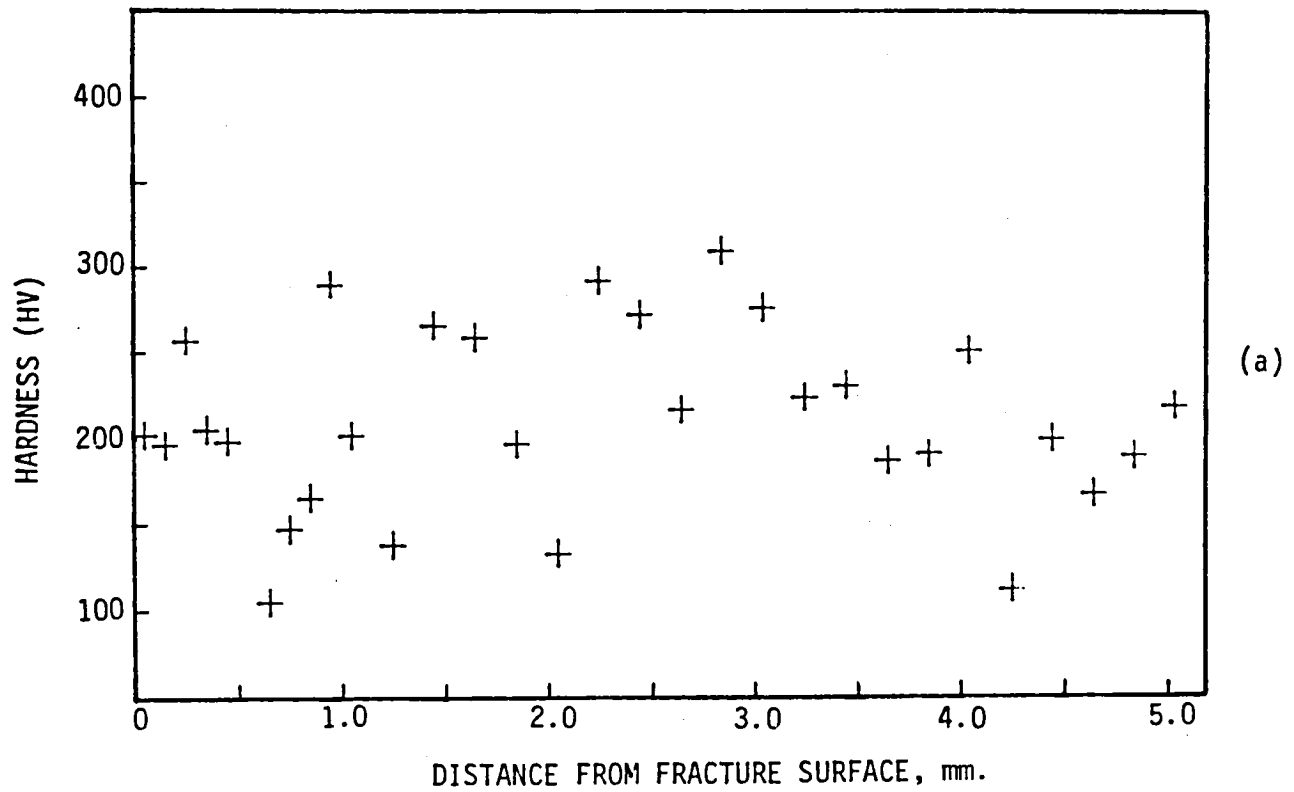


Figure 12. Hardness profiles along mid-thickness on cross sections (a) 3.5 mm., (b) 5 mm., (c) 7 mm., (d) 9 mm. from the notch.

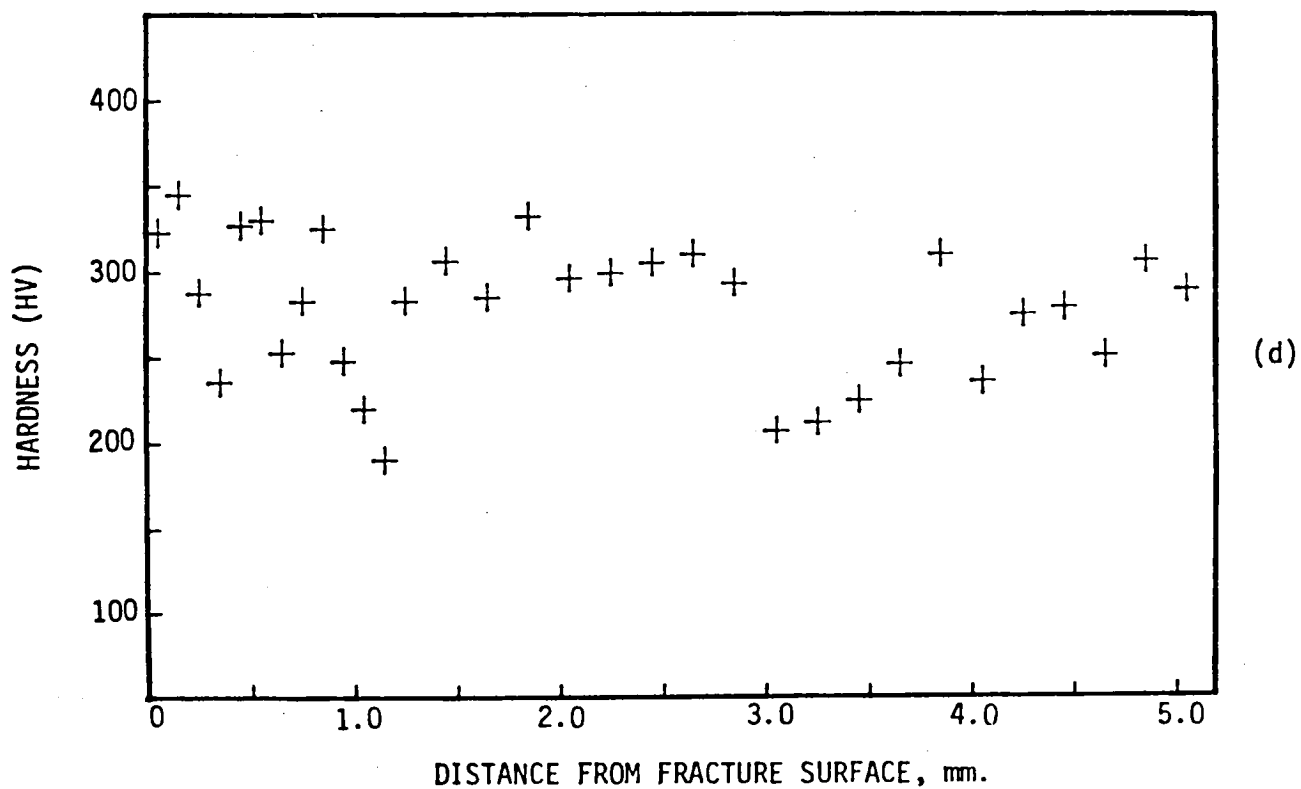
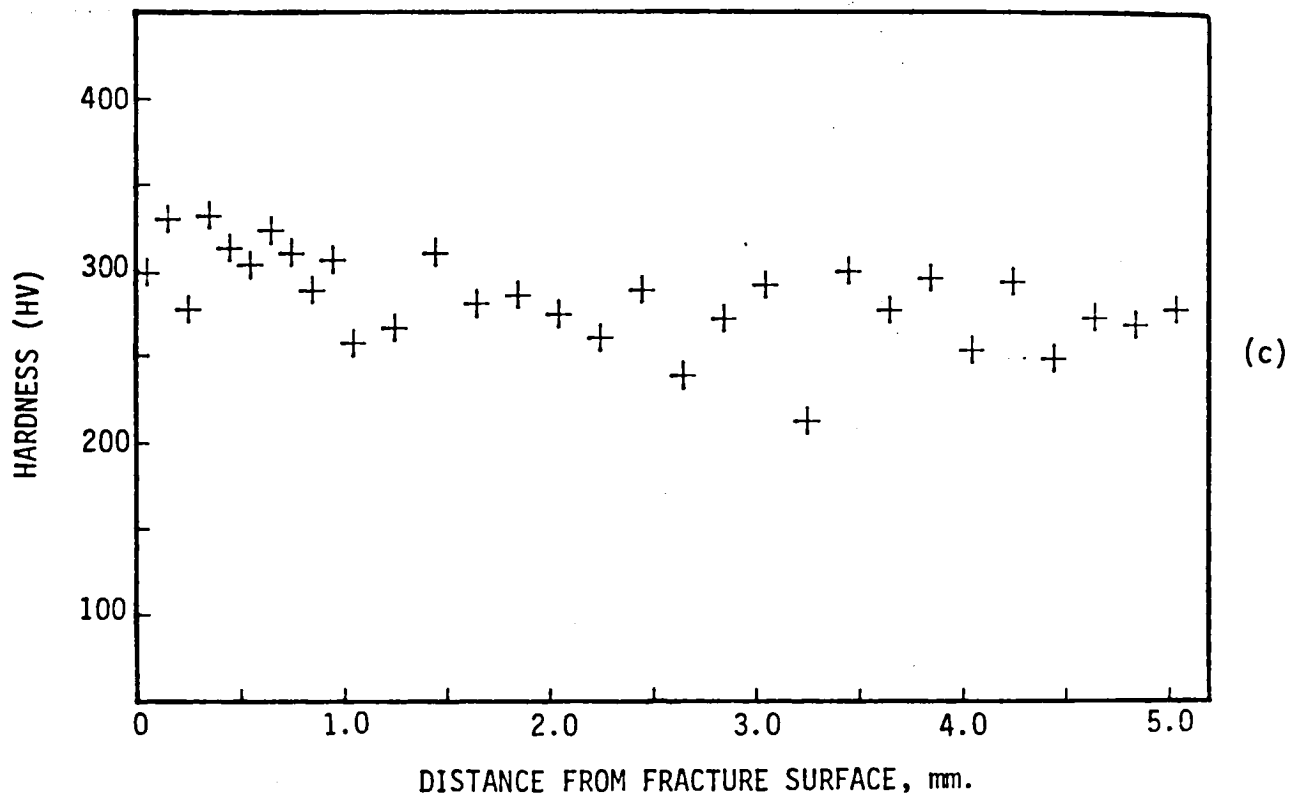


Figure 12, cont'd.

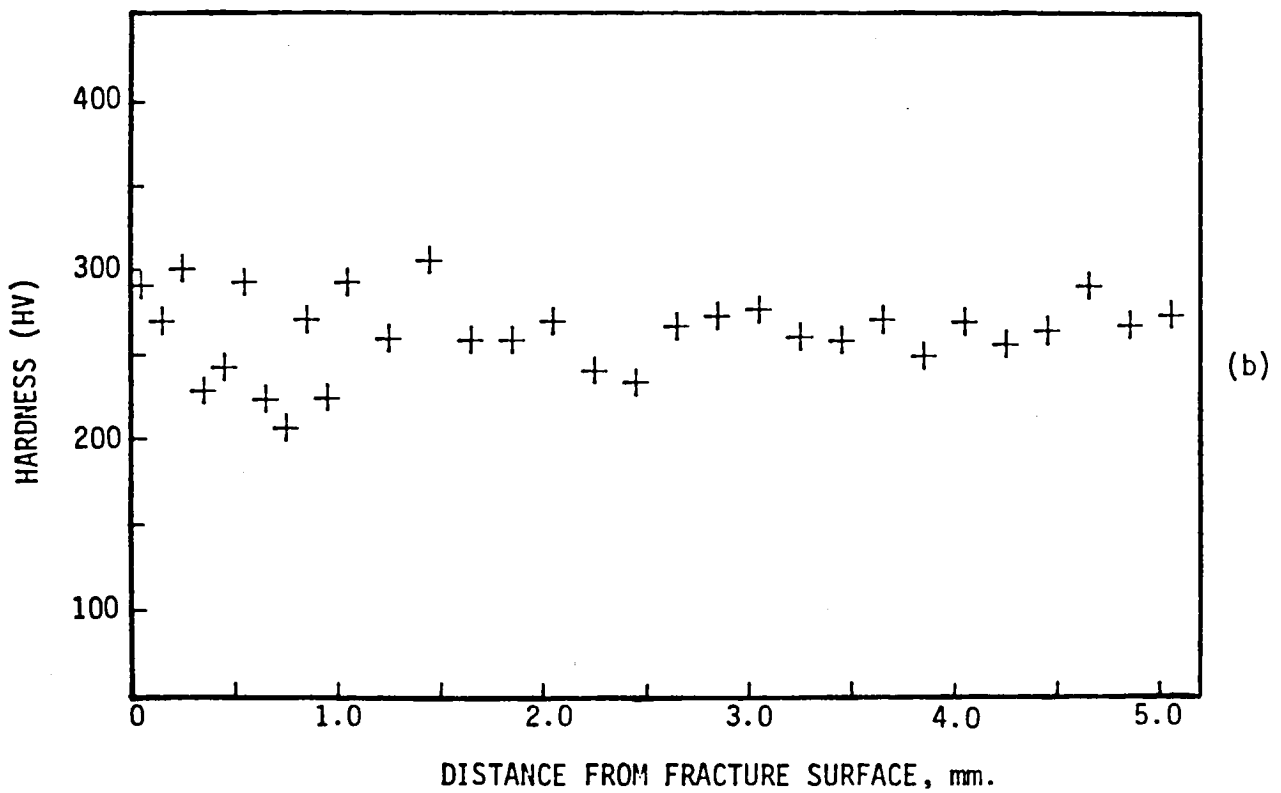
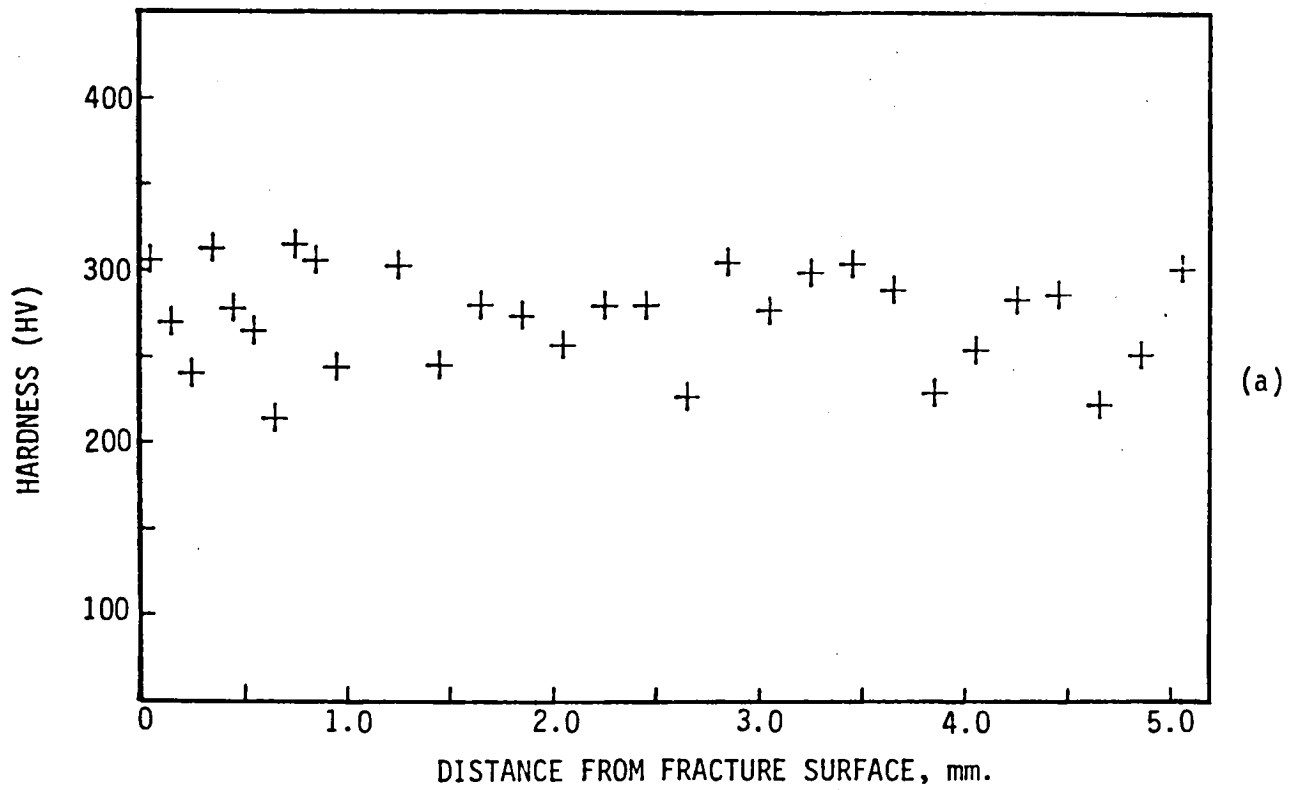


Figure 13. Hardness profiles along the edge on cross sections (a) 3.5 mm., (b) 5 mm., (c) 7mm., (d) 9 mm. from the notch.

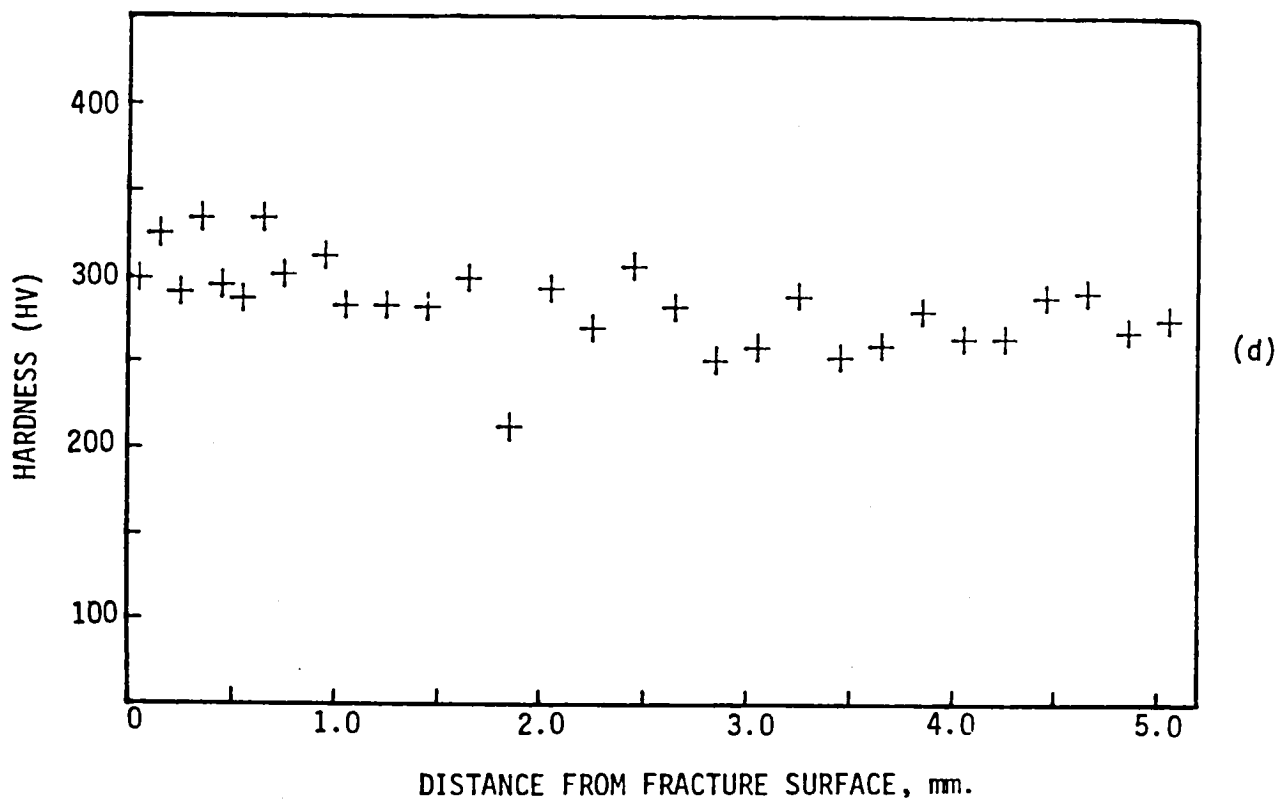
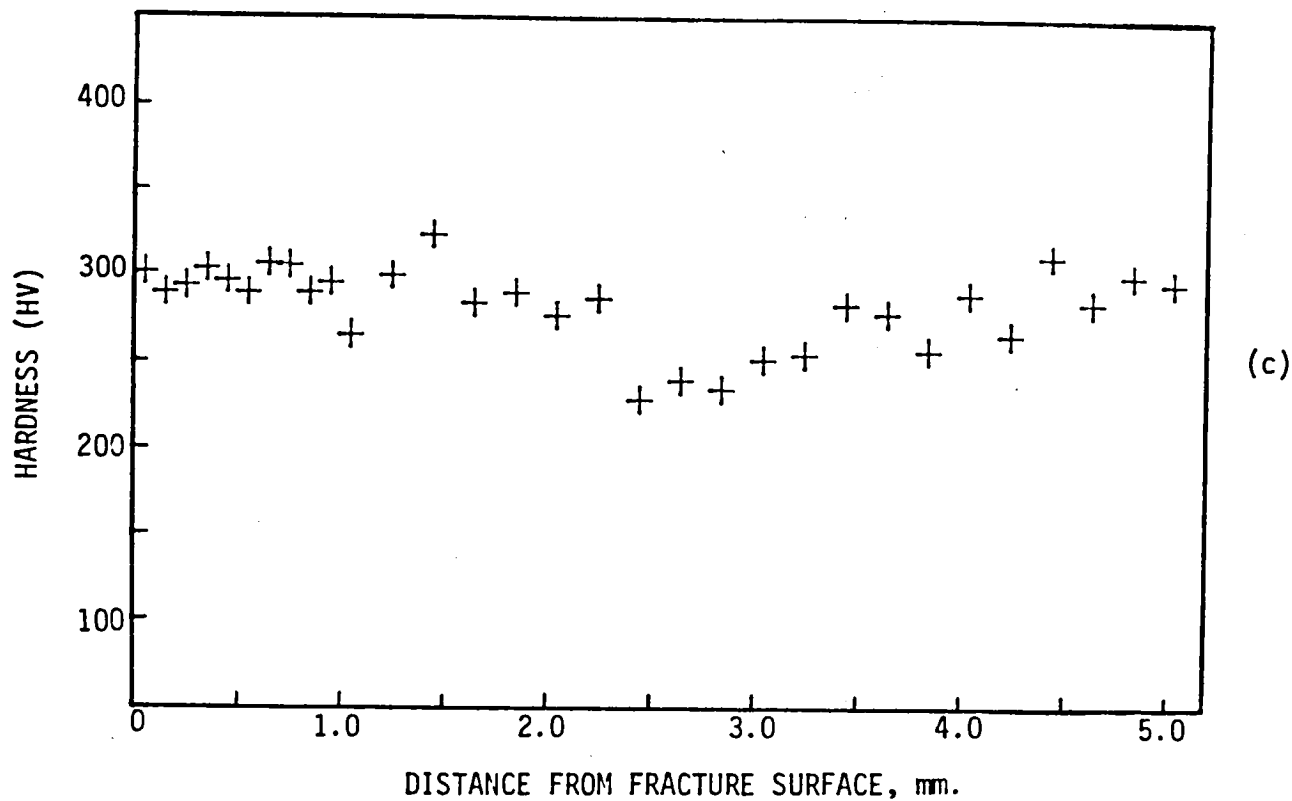


Figure 13, cont'd.

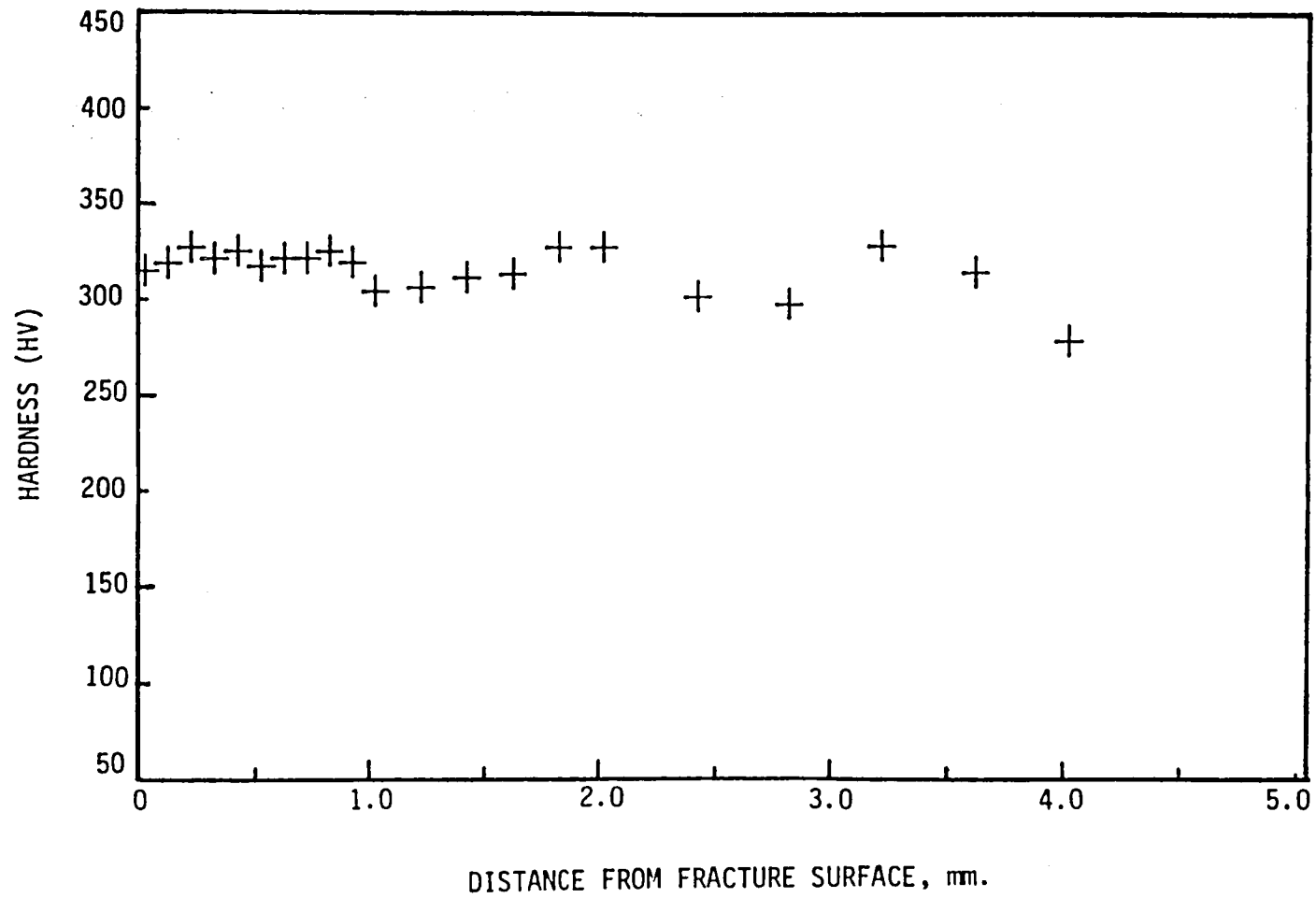


Figure 14. Hardness profile on the side surface of a fatigued specimen.



dislocation intersects the free surface may be relatively anodic or cathodic to certain etchants, particularly when impurity atoms are segregated to the dislocation. This results in the formation of etch pits, whose density on the surface is a sensitive indicator of the prior strain at or close to that surface (3,5,12). At low strains, one can observe etch pits from individual dislocations and a one to one correlation can be obtained. If the material is deformed to a large extent, pits are so dense that they can no longer be resolved; Etching in such a case, merely darkens the surface. Also, a one to one correlation is no longer given.

A vertical cross section similar to that used in hardness analysis was used in etching studies. The piece was aged at 160° C for 1 hour to allow the segregation of interstitials to dislocations for decoration purpose. Then it was etched electrolytically in Morris solution (25 g chromium trioxide, 133 cc acetic acid, 7 cc H<sub>2</sub>O). Etching occurs at approximately 5 v in 3-15 minutes without agitation. It is important to keep the solution temperature at about 20°c or below it. This method reveals the dislocation slip bands by prential etching.

The etching pattern of a vertical cross section is illustrated in Figure 15. The selectively attacked region is along mid-thickness in addition to the region underneath the fracture surface line and periodic bands down the cross section. These bands may correlate with the surface rumpling and may be associated with surface hardness patterns. However, etching effect suggests that the deformation caused by hot rolling is relatively large with respect to the damage induced by fatigue crack propagation.

#### RECRYSTALLIZATION TECHNIQUE

The deformed state is a condition of higher internal energy than the

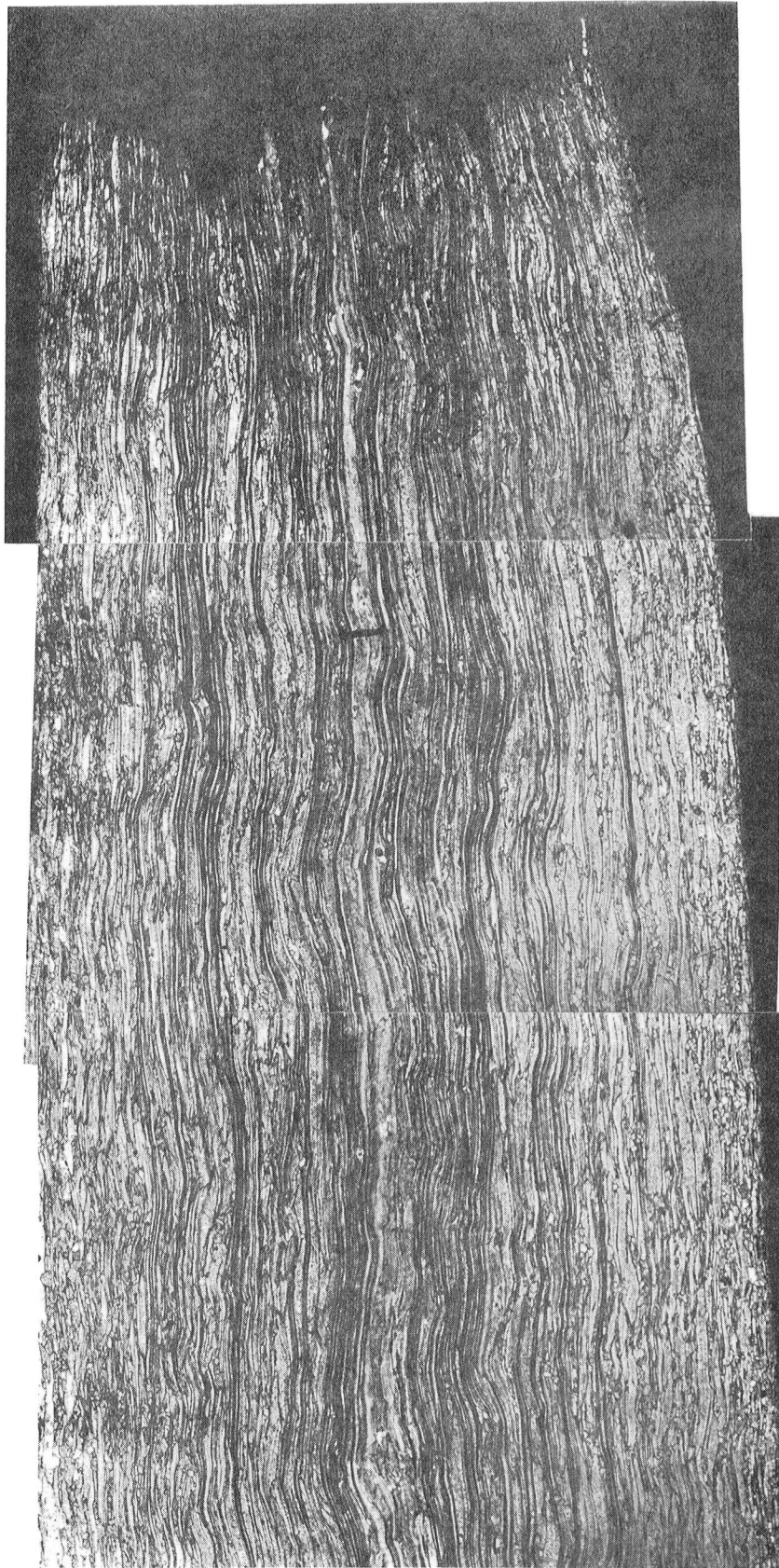


Figure 15. Etching pattern of a vertical cross section from a fatigued specimen.

undeformed state. Although the deformed structure is mechanically stable, it is thermodynamically unstable. With increasing temperature, the deformed state recovers from its unstable condition. Eventually, the metal softens and reverts to a strain free condition.

Recrystallization is the replacement of the deformed structure by a new set of strain-free grains. This is readily detected by metallographic methods and is evidenced by a decrease in hardness or strength. Recrystallization can be used as a technique to study the plastic zones of fatigue cracks. Among the variables that influence recrystallization behavior, the amount of prior deformation, temperature and time of annealing are significant. Time and temperature can be controlled during the heat treatment. Prior deformation is that of fatigue crack propagation for fatigued specimens and is expected to be a function of distance from fracture surface and notch.

For a given annealing condition (time, temperature), there is a critical amount of deformation for recrystallization to take place. The smaller the degree of deformation is, the higher is the required temperature (and/or longer is the annealing time) for recrystallization. The recrystallized grain size depends mainly on the degree of prior deformation and to a lesser extent on the annealing temperature. Above the critical deformation, the recrystallized grain size decreases with increasing prior strain.

The aspects of recrystallization listed above can be utilized in two different ways to study the plastic zones (13).

1. Step Annealing: A specific time and temperature can be used to recrystallize the regions which are deformed above a critical level (Figure 16a).

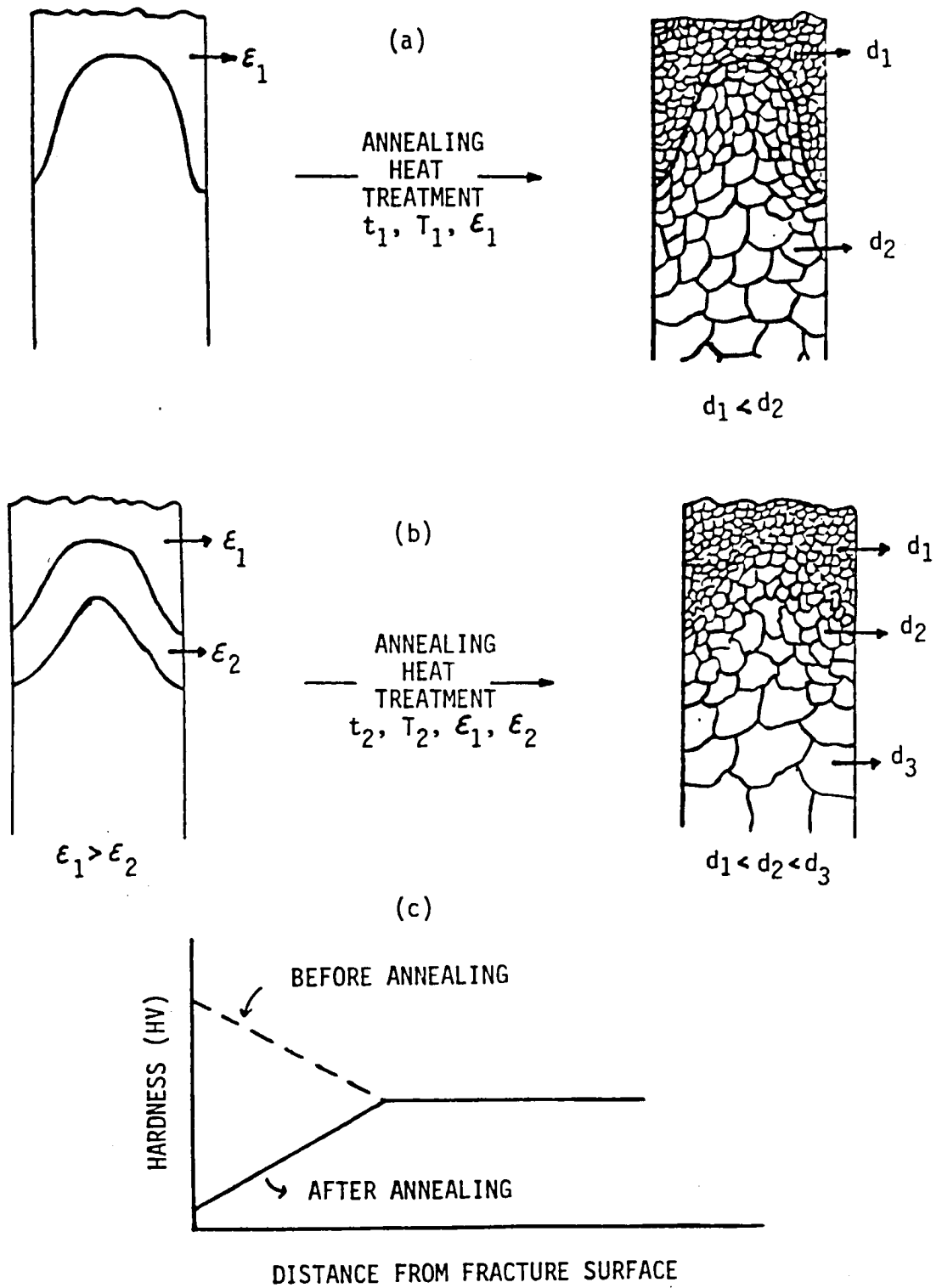


Figure 16. Recrystallization as a technique to study the plastic zones:  
(a) Step annealing, (b) Grain size, (c) Hardness.

2. Grain Size: Annealing heat treatment can be carried out under such conditions ( $t, T$ ) that the whole structure recrystallizes. In this case depending on the prior deformation the resulting grain size of different regions will be different (Figure 16b).

Hardness can also be used as an indication of recrystallization and can be coupled with step annealing technique for geometrical characterization of the plastic zone. In samples annealed after fatigue, the hardness gradients would be opposite to those obtained from fatigued specimens (Figure 16c).

As received material was found to recrystallize completely at temperatures above 1500°F. Vertical cross sections therefore, were annealed at temperatures ranging from 1200°F to 1450°F for 1 to 3 hours to allow selective recrystallization. In other words, the prior strain history of the material was accounted for, and regions with additional fatigue deformation were allowed to recrystallize during annealing heat treatment. Cross sections were then etched to examine the grain structure. Hardness measurements were also carried out on these cross sections to determine potential hardness gradients.

The optical micrographs of specimens annealed after fatigue are illustrated in Figures 17, 18, 19 and 20. Regions with relatively small and equiaxed grains are believed to have experienced a larger deformation. The fact that grain shape was elongated prior to annealing makes it possible to detect recrystallized regions because they have equiaxed grains.

Figures 17 and 18 illustrate the microstructures of two vertical cross sections 3 and 8 mm away from the notch respectively. The specimen was fatigued at  $P_{max} = 0.6 P_y$  and annealed at 1375°F for 2.5 hrs. The extent

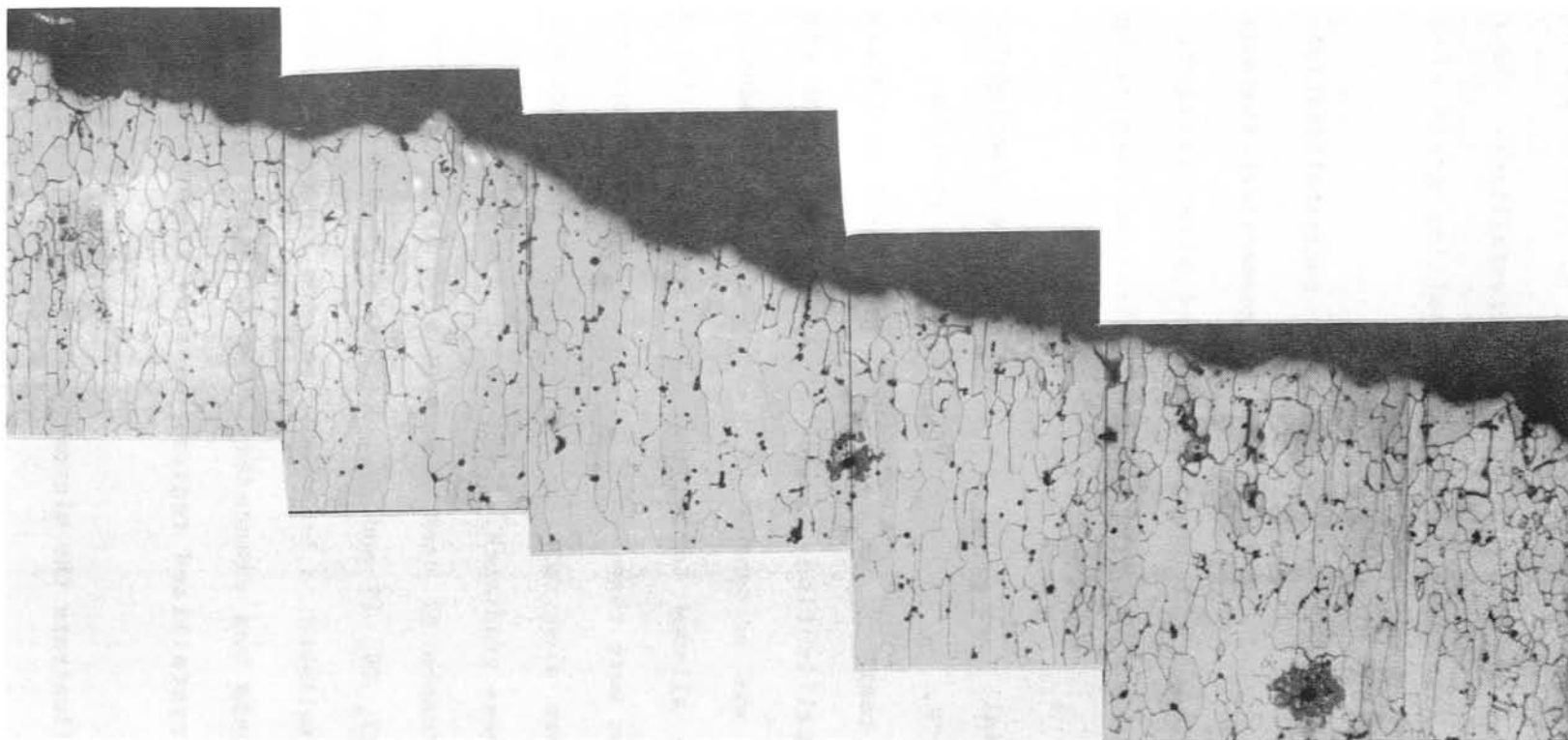


Figure 17. Microstructure of a vertical cross section 3mm. from the notch after annealing at 1375°F for 2.5 hrs.

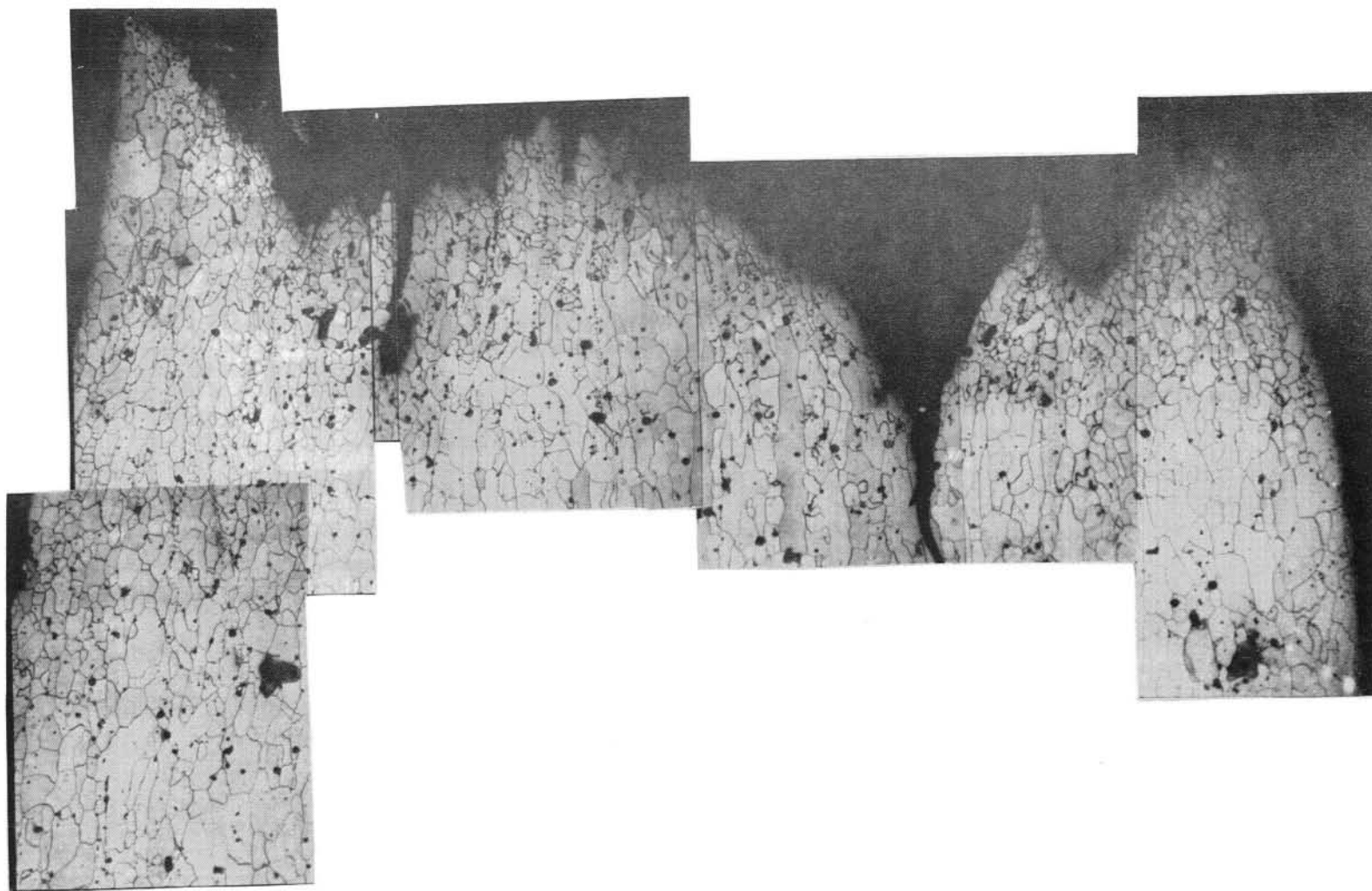


Figure 18. Microstructure of a vertical cross section 8 mm. from the notch after annealing at 1375°F for 2.5 hrs.

of recrystallization is larger on the cross section 8 mm away from the notch and this indicates that this section represents a higher deformation region.

Figure 19 represents the same conditions as in Figure 17 except that the annealing temperature was increased to 1400°F whereas the duration of heat treatment was 2 hrs. instead of 2.5 hrs. Temperature of annealing is a far more influential variable than time and its increase causes some recrystallization which was not observed in Figure 17.

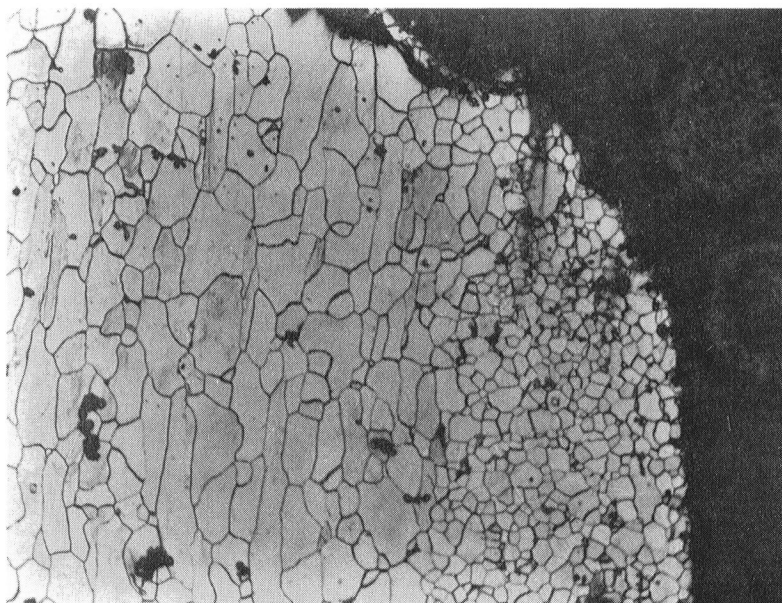


Figure 19. Microstructure of a vertical cross section 3 mm. from the notch, after annealing at 1400°F for 2 hrs.

Another micrograph taken from the side surface is shown in Figure 20. The grain size is very large next to the fracture surface edge and gets smaller as we go away from the edge. It could be that grain growth started along the edge whereas recrystallization was still in progress in the rest of the surface. This explanation applies to a very thin surface layer



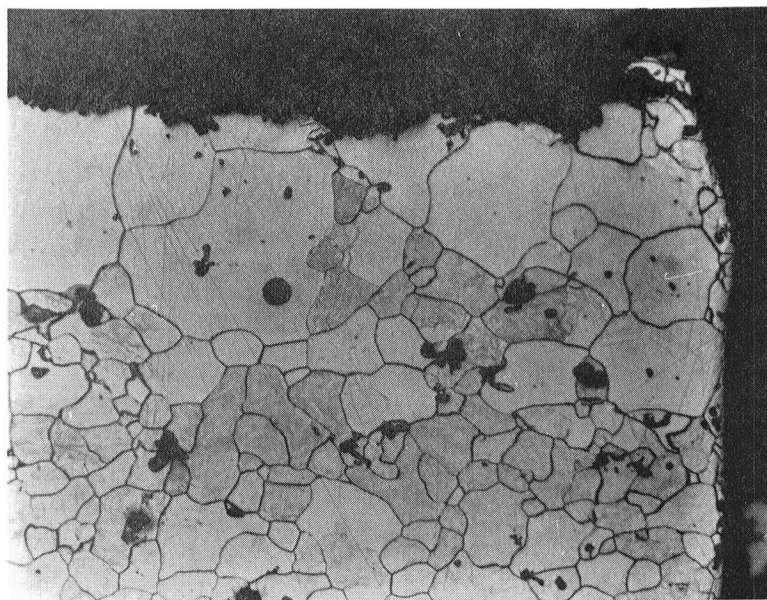


Figure 20. Microstructure of a side surface after annealing.

which might have undergone heavier deformation.

Hardness analysis on annealed samples has shown that under the same annealing conditions; the hardness level of the cross sections further away from the notch (heavily deformed) is lower than closer to it (lightly deformed). This is opposite to what was found from hardness analysis on fatigued but not annealed specimens. More deformed cross sections have been influenced by recrystallization to a greater extent and the hardness drop has been larger. The variation of hardness within short distances, i.e. scatter, was also reduced. Examples to the above are illustrated in Figure 21.

#### COMPRESSION METHOD

Cross sections of fatigued specimens can be compressed in the transverse direction to about their yield strength. Because of residual back stress on dislocations, previously active slip systems can pop out of

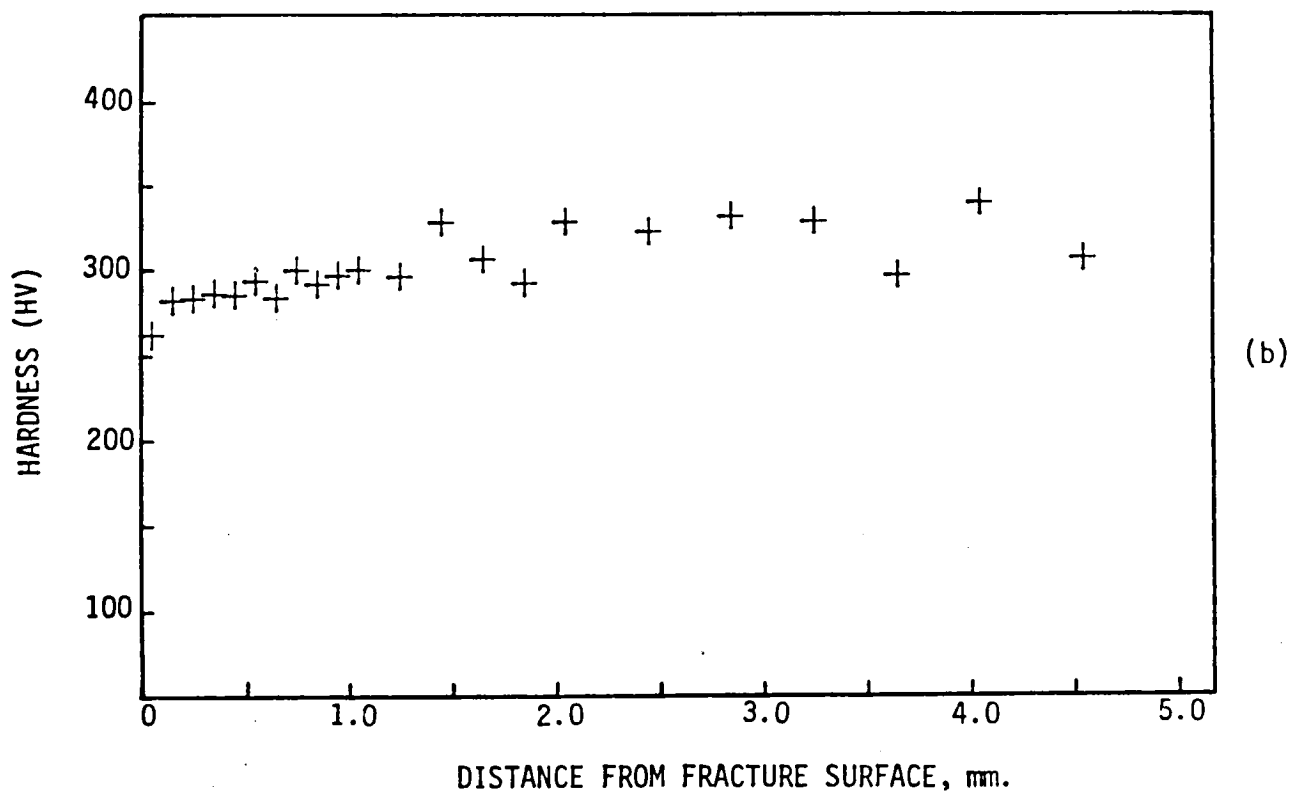
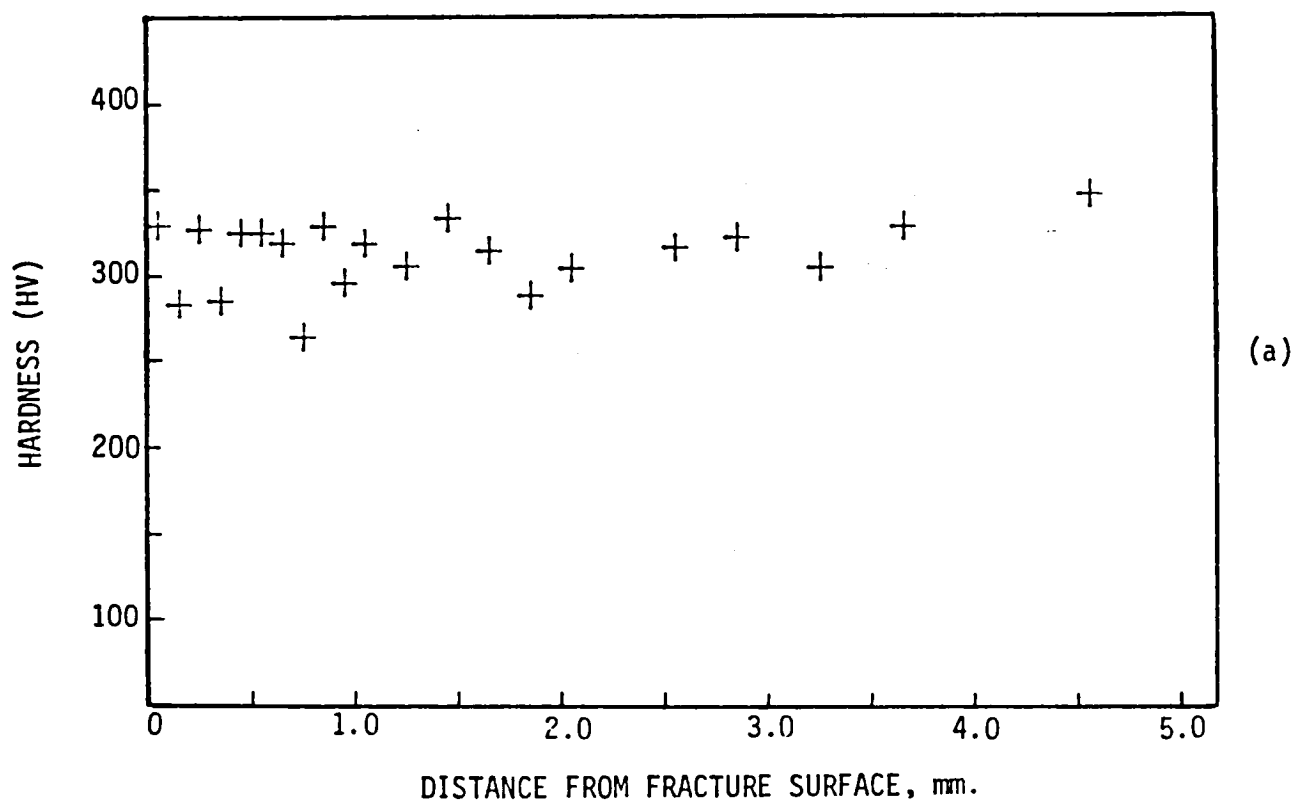


Figure 21. Hardness profiles along mid-thickness on a vertical cross section (a) 3 mm., (b) 8 mm. from the notch, after annealing at 1375°F for 2.5 hrs.

the polished cross-sectional surface, and it permits to observe the evolution of slip lines (14). The method relies on the fact that the microstructure contains residual stresses in fatigued specimens, whereas it is strain-free before fatigue. For non-deformed metals, it takes a stress above the yield point to activate slip to produce permanent deformation. However a lower stress can accomplish this in the plastic zone of a fatigued specimen.

Fatigued specimens were sectioned to produce cross sections at 90 degrees as well as cross sections at some angle with respect to the fracture surface. These cross sections were polished to mirror quality, and the specimens were compressed in the transverse direction to different stress levels to initiate slip. For comparison, these tests were repeated on as received material.

The compression load was applied in two fashions: (i) Fatigued and as received specimens were loaded to the same level and then examined carefully with optical microscope. The load was high enough to produce sufficient slip activity on the polished surface. The density of slip lines was to be compared in this test. (ii) Fatigued and as received specimens were loaded until roughness initiated on the free surface of the cross section. During the compression test, the surfaces were observed with a magnifier. The load at which roughness initiated on the polished surface was to be compared for the two kinds of specimens.

For an evaluation of compression tests results, it was assumed that the yield strength of Fe-2.6 Si alloy in compression is equal to that in tension. Fatigued specimens have undergone permanent shape changes at lower stress levels than the as received specimens. At low stresses, extensive roughness in the form of surface rumpling which correlated with

grain structure was observed. However individual slip lines were difficult to find unless the stress was increased to about the yield point. An example of slip lines that evolve on a polished surface upon compression is illustrated in Figure 22. The stress level at which any surface activity

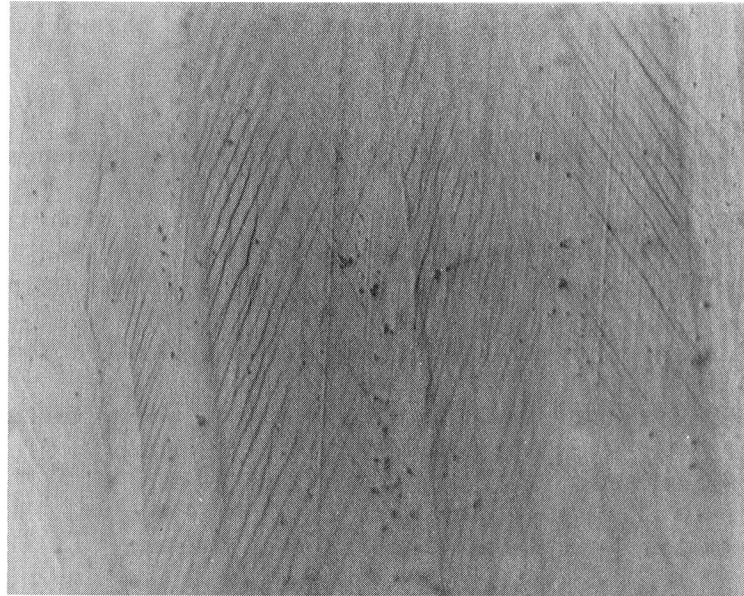


Figure 22. Slip lines that evolved on a vertical cross section of a fatigued specimen when compressed to about its yield point.

starts is believed to be a function of prior strain history of the specimen. These tests have confirmed that it takes less stress to activate slip systems in a previously deformed specimen.

#### TRANSMISSION ELECTRON MICROSCOPY

TEM techniques can be employed to quantify the damage through the thickness as a function of location with respect to fracture surface and notch. Thin foils at different depths from the fracture surface and at different distances from the notch can be examined to evaluate the amount of damage in terms of dislocation density and cell wall thickness.

Dislocations are often distributed rather homogenously in the very early stages of fatigue and tend to form heterogeneous configurations, clusters before a cell structure develops (15, 16). However the application of TEM techniques for geometrical characterization of the plastic zone is not practical.

Thin foils were prepared from right underneath the fracture surface next to the notch, as shown in Figure 23. A thin foil was obtained from the as received material with the same relative position for comparison purposes. These foils were examined with a Philips 400T microscope at 120 KV.

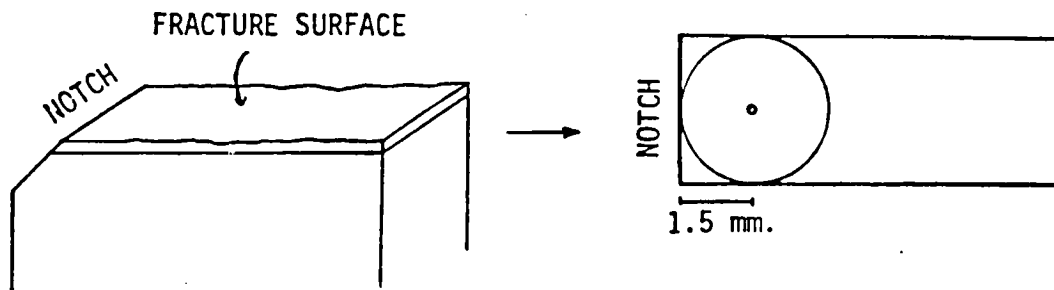
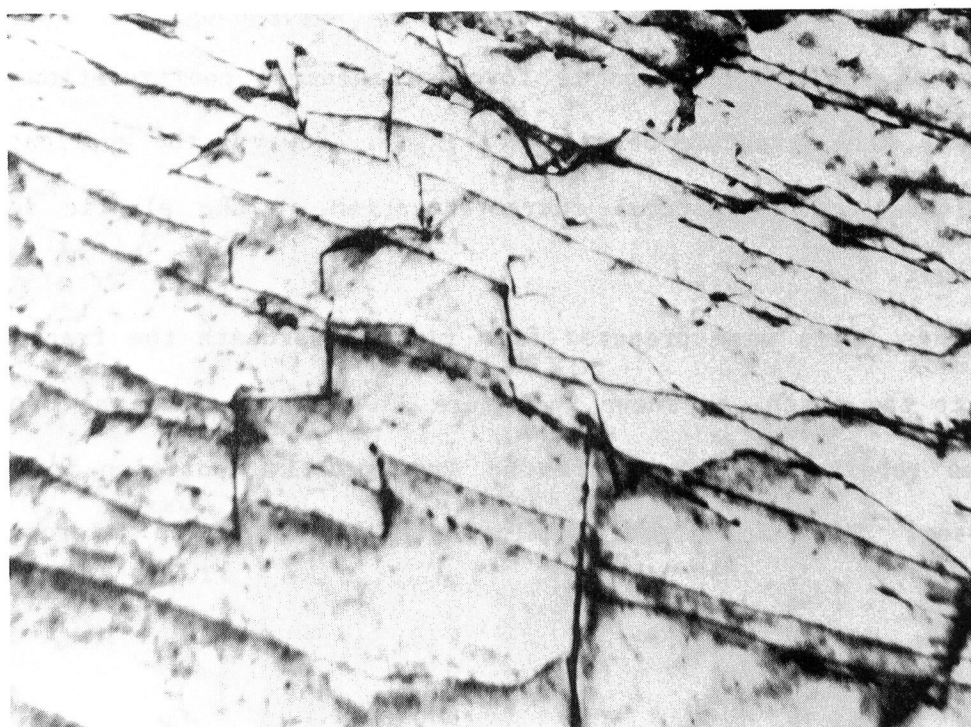
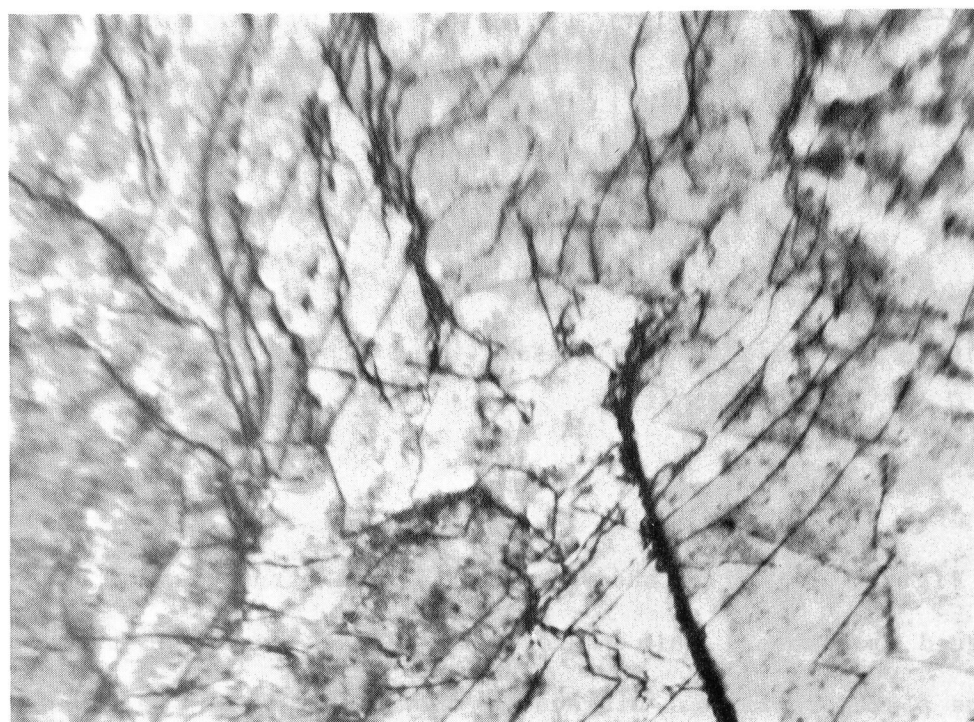


Figure 23. Illustration of sampling of thin foils examined in this investigation.

Figures 24 and 25 show the dislocation structures of as received and fatigued specimens. Thin foils in both cases represent the mid-thickness of the plate specimens. Dislocation density of the as received material is very high at mid-thickness and has not increased due to fatigue. In fact, the electron micrographs suggest that it might have decreased. The cyclic

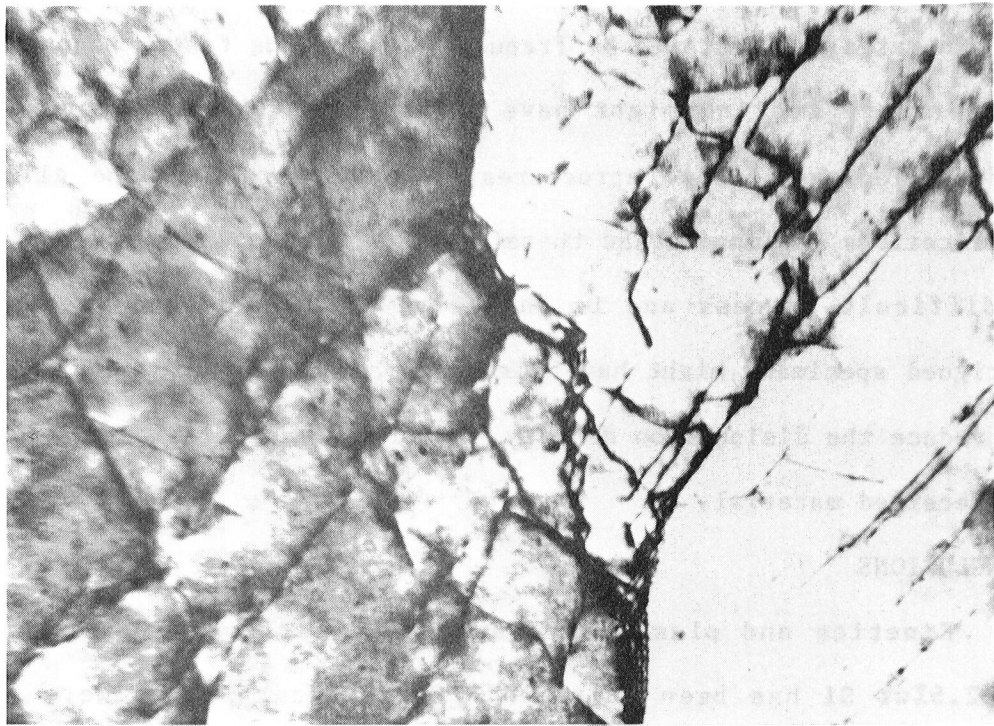


a

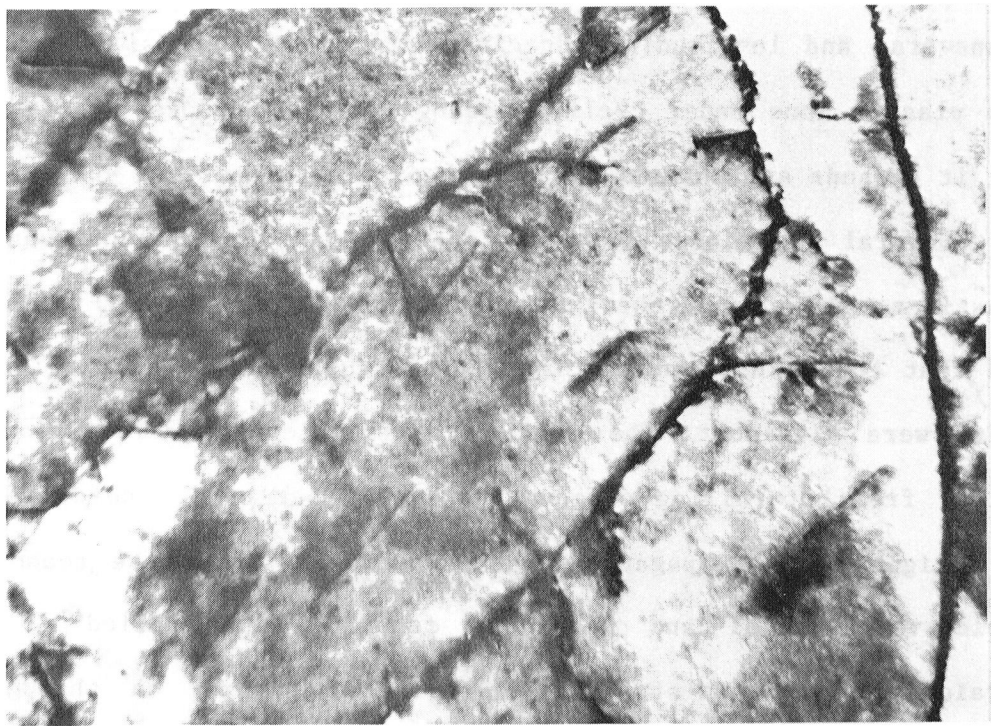


b

Figure 24. Dislocation structure of as-received material.



a



b

Figure 25. Dislocation configurations in fatigued specimen. Note the sub-boundaries in (b).



strain rates, as dictated by frequency of fatigue tests, together with room temperature testing might have favored the low temperature regima of deformation for b.c.c. structures. In this regime, the glide of screw dislocations is impeded and therefore the multiplication of dislocations is a difficult process and is unlikely. Some subboundaries observed in fatigued specimens might have served as a sink for dislocations and helped to reduce the dislocation density. Such subboundaries were not observed in as received material.

#### CONCLUSIONS

Kinetics and plasticity aspects of fatigue crack propagation in Fe-2.6%wt Si has been obtained. Crack growth rates were found to be slightly higher in longitudinal direction as would be expected from the inferior tensile properties in this direction. Plastic zone evolution in transverse and longitudinal specimens has shown many similarities. Crack tip plastic zone under cyclic loading conditions does not only translate but it expands and changes shape with crack propagation.

Several techniques were employed in the through-thickness study of plastic zones. Due to the fact that specimens were in hot-rolled condition and that they exhibited laminar grain structure the interpretation of results were difficult. The degree of mid-thickness deformation in particular, from hot-rolling process was comparable to the deformation induced by fatigue crack propagation. It is believed that these techniques would yield very useful and meaningful results when applied to completely strain-free, uniform-structure materials. A study on through-thickness characterization of plastic zones in annealed (strain-free) silicon-iron is underway.



## References

1. R.N. Wright and A.S. Argon, Metallurgical Transactions, (Vol. 1) 1970 p.3065.
2. C.E. Richards, Acta Metallurgica, (Vol. 19) 1971, p. 583.
3. G.T. Hahn, R.G. Hoagland and A.R. Rosenfield, Metallurgical Transactions, Vol. 3. 1972, p. 1189.
4. D.L. Davidson and J. Lankford, Journal of Engineering Materials and Technology, 98, 1976, p. 24.
5. K. Tanaka, M. Hojo and Y. Nakai, Materials Science and Engineering, 55, 1982, p. 85.
6. A. Chudnovsky, NASA Report, December 1983.
7. C. Bathias and R.M. Pelloux, Metallurgical Transactions, 4, 1973, p. 1265.
8. A. Pineau and R.M. Pelloux, Metallurgical Transactions, 5, 1976, p. 1103.
9. A Saxena and S.D. Antolovich, Metallurgical Transactions, 6A, 1975, p. 1809.
10. A.H. Purcell and J. Weertman, Metallurgical Transactions, 5, 1976, p. 1805.
11. C. Loye, C. Bathias, D. Retali and J.C. Devaux, ASTM STP 811, 1983, p. 427.
12. K. Tanaka, M. Hojo, and Y. Nakai, ASTM STP 811, 1983, p. 207.
13. E. Hornbogen, E. Minuth and St. Stanzl, Materials Science and Engineering, 43, 1980, p. 145.
14. Metals Handbook.
15. H. Mughrabi, Dislocations and Properties of Real Materials, The Institute of Metals, London, 1985.
16. M. Klesnil and P. Lukas, Proc. 2nd. Int. Conf. Fracture, (1969), p. 725.

1. Report No. <b>NASA CR-175115</b>		2. Government Accession No.		3. Recipient's Catalog No.	
4. Title and Subtitle <b>Fatigue Crack Layer Propagation in Silicon-Iron</b>				5. Report Date <b>May 1986</b>	
				6. Performing Organization Code	
7. Author(s) <b>Y. Birol, G. Welsch, and A. Chudnovsky</b>				8. Performing Organization Report No. <b>None</b>	
				10. Work Unit No.	
9. Performing Organization Name and Address <b>Case Western Reserve University Cleveland, Ohio 44106</b>				11. Contract or Grant No. <b>NAG 3-223</b>	
				13. Type of Report and Period Covered <b>Contractor Report</b>	
12. Sponsoring Agency Name and Address <b>National Aeronautics and Space Administration Washington, D.C. 20546</b>				14. Sponsoring Agency Code <b>505-63-81</b>	
15. Supplementary Notes <b>Final report. Project Managers, Bernard Gross and Anthony M. Calomino, Structures Division, NASA Lewis Research Center, Cleveland, Ohio 44135.</b>					
16. Abstract <b>Fatigue crack propagation in metal is almost always accompanied by plastic deformation unless conditions strongly favor brittle fracture. The analysis of the plastic zone is crucial to the understanding of crack propagation behavior as it governs the crack growth kinetics. This research was undertaken to study the fatigue crack propagation in a silicon iron alloy. Kinetic and plasticity aspects of fatigue crack propagation in the alloy were obtained, including the characterization of damage evolution.</b>					
17. Key Words (Suggested by Author(s)) <b>Cracks Fatigue crack propagation</b>			18. Distribution Statement <b>Unclassified - unlimited STAR Category 39</b>		
19. Security Classif. (of this report) <b>Unclassified</b>		20. Security Classif. (of this page) <b>Unclassified</b>		21. No. of pages <b>46</b>	
				22. Price* <b>A03</b>	



National Aeronautics and  
Space Administration

**Lewis Research Center**  
Cleveland, Ohio 44135

Official Business  
Penalty for Private Use \$300

SECOND CLASS MAIL

ADDRESS CORRECTION REQUESTED



Postage and Fees Paid  
National Aeronautics and  
Space Administration  
NASA-451

NASA Langley Research Ctr  
Attn: Library  
MS-185  
Hampton, VA 23665

**NASA**

---